Year Two: The Absorption of Space Radiation with Development in Shielding Materials

High School Senior Research Project

By: Devon Madden

Table of Contents

Background:

PROBLEM STATEMENT

Astronauts and Electrical Engineers needs an improved shielding material for protection against high energy particles from space. This becomes of importance regarding the future exploration of deep space and possible missions to Mars where human exposure to the events in space can cause not only biological issues but also psychological damage as well. Another aspect to recognize is the usage of satellite systems in Earth's orbit, where high energy particles can also deposit and cause damage to the electronic components comprising the lifetime or functionality of a device for communication requirements on Earth. In this section, background will be covered on Galactic Cosmic Rays, the Fermilab Scintillation detector, and shielding methods as well.

GALACTIC COSMIC RAYS

From the *Space Weather Prediction Center* at *the National Oceanic and Atmospheric Administration* (NOAA) defines Galactic Cosmic Rays (GCRs) as highly energetic particles that constantly strike Earth's atmosphere from supernovas, the sun, and other explosive events in deep space. These particles travel with both high speeds and energy levels; they can be divided into primary and secondary Cosmic Rays ("Galactic," n.d.). Primary Cosmic Rays' energy levels can vary from 10^9 electronvolt (eV) to 10^{20} eV explaining how these particles are able to last such long distances and remain stable. Primary Cosmic Rays particles include the proton and Hydrogen nucleus originating from space events such as black holes, neutron stars, and the Big Bang (Kliewer, n.d.). Once these particles travel to Earth, the planet's atmosphere and magnetic field reduce primary particles to secondary Cosmic Rays that are less dangerous and can be detected on Earth (“Galactic,” n.d.). Exposure to Cosmic Rays and ionizing radiation from outer space has been linked to both human and electronic related complications in NASA related missions.

FERMILAB QUARKNET DETECTOR SYSTEM

The secondary particles produced in Earth’s atmosphere travel to the surface of Earth and can be detected with sensitive instruments (“Galactic,” n.d.). As explained from the Fermilab National Accelerator Laboratory, a scintillation detector was first developed in 1999 by Sten Hansen to conduct a muon lifetime study using a scintillator mated to a photomultiplier tube and an analog to digital data acquisition (DAQ) board. Since then schools and colleges wanted to conduct Cosmic Ray experiments and the scintillation detector was adapted and improved in recent years to be an affordable instrument for students to conduct particle physics research at ease (Cecire, 2002). Named the Fermilab Quarknet Cosmic Ray detector system, the device was developed by the company Fermilab to, “ create a simple, low-cost cosmic ray detector for use in educational settings” (p. 1). The detector can be used for Cosmic Ray experiments including: flux monitoring and muon lifetime calculations to better study and understand high energy particles from space. The current detector is composed of the following main components: scintillator, Photomultiplier tube, and DAQ board; it should be noted that other materials are required to run the detector as well, but these are the highlights for how it works. The scintillation paddle is made of a special type of plastic called a scintillator (Lofgren, 2001). As explained by *McMaster University,* the organic scintillator used in the detector absorbs the energy from an incoming charged particle and excites the particle into an excited state causing a photon to be emitted between energy levels (Byun, n.d.). The Photomultiplier tube (PMT) then detects the created photon by its photosensitive material converting it into an electron. The electron is then relayed in the system to create more electrons or enough voltage to send a signal to the DAQ. Finally the DAQ, records the timing of the pulses and the particle count for the computer to receive for data analysis (Lofgren, 2001).

CHRONIC EFFECTS ON HUMANS

NASA's *Lyndon B. Johnson Space Center* predicted using models on risks and uncertainties built upon the interaction of GCRs in matter and data regarding studies on different forms of cancer. The Risk of Exposure Induced Death (REID) or the chances of developing a chronic illness from exposure to space radiation, cardiovascular diseases and various types of cancers, are 3 times higher than the NASA safety limit. This is seen in the document's Figure 2, which shows how exposure to deep space the %REID peak is at 1.7 % compared to exposure to high energy particles on the ISS or on Mars when it reaches a particle at 1000 Z^{*2}/β^2 (Cucinotta, Kim, Chappell, & Huff, 2013). *The Journal of Radiation Research* published an article also on the relationship between Cosmic Rays and damage to the human body (Ohnishi, 2016). Researchers placed animal cells on the International Space Station to analyze the effects of exposure to the space environment. It was found that heavy ion particles caused DNA damage to tested cells with a dose of 94.5 mSv in the 133 day period (p. i42).

Exposure to radiation from outer space has also been linked to psychological damage. As the *University of Rochester Medical Center* conducts a study proving the correlation between exposure to GCRs and the early onset of Alzheimer's disease. Using a small mice population, half of the test subjects were exposed to an iron ion beam from NASA's Space Radiation Lab. The control and exposed groups were then tested in a series of behavior activities, followed by bisecting the brains to examine Amyloid Beta (Aβ) plaque buildup in the brain's tissue. "Monitoring plaque progression in vivo has been used to gauge disease severity…" (p. 1). The study's results showed little effect of radiation exposure in behavioral testing when compared to the controlled, however a larger plaque size was found with dying the brain tissue of mice exposed to the iron ion beam. This study suggests there are effects on the brain from exposure to GCRs in space (Cherry et al., 2012).

FUNCTION FAILURE IN SATELLITE SYSTEMS

Space radiation has also been shown to cause technical damage to the operation and lifespan of many satellite systems in Earth's orbit. As discussed by the *American Institute of Physics,* there is a growing need of electronic components to be immune to the effects of space radiation when placed in orbit. This is due to the reliance of satellite systems in space to provide services for communication, entertainment, and information (Tripathi, 2011). The *International Conference on Microelectronics,* explain how protons and electrons can penetrate the shielding of a satellite or spacecraft causing ionization events in the device. For instance, if a Cosmic Ray enters a sensitive area on an integrated circuit, the entire satellite system can fail due to the energy deposited causing, "single-particle-induced latchup…, burnout, or dielectric rupture" (p. 2). This process can cost excess money for companies who invested in system, the transportation; as well as the inconvenience it may have caused to people on Earth regarding communication failure (Fleetwood & Winokur, 2000).

CURRENT AND FUTURE SOLUTIONS

As stated by NASA, the only option for shielding against harmful space radiation now is by shielding materials. “There are two ways to shield from these higher-energy particles and their secondary radiation: use a lot more mass of traditional spacecraft materials, or use more efficient shielding materials” (Frazier, 2015). Density and thickness of a substance are two factors that can affect how much radiation is absorbed regarding shielding against high energy particles. Thickness is useful for particles that require a longer interaction length and where mass or size doesn’t matter. Density is important to a substance because there are more atoms and electrons to interact with high energy particles; similar to a spider web, the quantity of strands in the web makes it more difficult for a fly to pass through the spider’s trap. As explained from the Physics Department at *California State Polytechnic University,* Lead is effective in absorbing radiation because of its density (“How,” 2009). Where Lead has a density of 11.35 g/cm^3 compared to Aluminum, 2.7 g/cm^3, and Hydrogen, 0.09 g/cm^3 (“Chemical,” n.d.). High density materials work the same, when a high energy particle passes through the Lead it interacts with the cloud of electrons around each atom. This is known as the attenuation, decrease in intensity, of radiation with matter (Siegel, 2015). The electron absorbs the energy of the particle and becomes, “a safe form of energy and a way of neutralizing the effects of the radiation” (“How,” 2009). Other high density materials include: Tin, 7.31 g/cm^3; Steel, 7.75-8.05 g/cm^3 (“Density,” 2016); Copper, 8.96 g/cm^3; Silver, 10.5 g/cm^3; and Gold, 19.32 g/cm^3 (“Chemical,” n.d.).

NASA has been working on other ways of protecting astronauts and systems from the harmful effects of GCRs. In an article called, “Real Martians: How to Protect Astronauts from Space Radiation on Mars,” explains the potential of other materials and methods of reducing the damage induced by ionizing radiation in space. Hydrogen has been looked at as a possible shield by surrounding a spacecraft in a layer of water or using polyethylene the same plastic used in common household items. Although these ideas are promising, they are difficult to integrate into the structure of a spacecraft or suit. “One material in development at NASA has the potential to do both jobs: Hydrogenated boron nitride nanotubes—known as hydrogenated BNNTs…” (Frazier, 2015). Hydrogenated BNNTs are composed of tiny tubes of the elements Carbon, Boron, and Nitrogen; where Hydrogen is located in the spaces in the tubes. Combining these components increases the material ability to be structurally adaptable and effective for shielding. In the future, other ideas could be potentially developed to protect against harmful radiation including: force fields, spacewalks time minimized on different planets, and medication to counteract the effects of radiation exposure (Frazier, 2015).

CLOSING STATEMENTS

From this research it has been revealed that both astronauts and electrical engineers need an improved method for shielding against the harmful effects of space radiation. This was evident by looking into the effects of Galactic Cosmic Rays on both humans and satellite systems. Where exposure to space radiation has been linked to the development of chronic illnesses including various types of cancer, cardiovascular diseases, and development of mental disabilities like Alzheimer's disease. These reasons have pushed organizations like NASA to develop more effective shielding given their plans for space exploration with astronauts to Mars and beyond. Various solutions are discussed including: developing Hydrogen based shields, electromagnetic force fields, and medication to reduce the effects of ionizing radiation in the space environment. It can be stated based on this information, that for any long term mission beyond Earth's orbit will not be successful without development in space radiation shielding methods.

Introduction:

The purpose of the project is to determine or develop a more effective shielding material for use in space related applications. The material that is developed must be able to shield or absorb at least half of the incoming events. This number is determined from the total events occurring in the environment without any shielding material present within the scintillation detector for the 24-hour period of experimentation. The shielding material that is developed must also be safe to use, which means that it isn't radioactively decaying, producing dangerous radiation alone like Technetium (Winter, n.d.). The material can't be poisonous or toxic such as Lead when being handled or exposed to the environment ("Material," 2014). The material being developed must also be light and sturdy to use. Lead and concrete may be effective shielding material against radiation but requires a large thickness or mass to be used which wouldn't be acceptable for spacecrafts and satellites.

For the experiment, the control will be the scintillation detector running for 24 hours in a stationary environment. This will provide the number of muon events in a day based on the current environment being used for data collection. The count from the control section will also help, as mentioned above, to compare the number of events striking earth without any protection to the trials with different shielding materials in between the two detector paddles. To validify or reject last year's results, the student researcher will test the effectiveness of the shielding materials used previously in data collection to determine if Lead is the most effective material compared to Polyethylene and Aluminum. After researching potential materials to use for this current year's study, the student will use the knowledge he or she gained to develop a material compound to be the most effective against the incoming events. This will be done by layering the materials that demonstrate the most useful characteristics including density. Hopefully from the research found and the material developed tested in the detector system, the student researcher is able to discover a more effective shielding material to absorb muon events.

Astronauts and NASA engineers needs improved shielding material because of the harmful effects of high energy particles from Cosmic Rays. In the biological aspect, humans are affected both physically and psychologically (Cucinotta, Kim, Chappell, & Huff, 2013). Physical damage includes: circulatory disease, cancer, and other illnesses; the early onset of alzheimer's can result from radiation from space (“Space,” 2013). Technologically, electronic systems and satellites exposed to ionizing radiation face damage or in operation when the particles pass through the system (Fleetwood & Winokur, 2000). Developing a more effective shielding material becomes important when discussing the future of manned missions to space. If companies such as NASA or SpaceX plan to explore Mars or deep space with manned or unmanned shuttles, better radiation protection will be required to ensure the safety and the proper operation of future missions.

Materials List:

- Quarknet Cosmic Ray Detector
- Computer with PuTTY
- Polyethylene Sheet (12” x 12” x 1/32”)
- Gold Leaf Packet (48 sheets)
- Silver Leaf packet (12 sheets)
- Mill Finished Steel sheet metal (12” x 18” x 0.016”)
- Poster Board (22” x 28”)
- 3D Printer Supports
- Electronic Scale Balance
- Aluminum Foil (12 ¼” x 10 ⅛”)
- Lead Foil (12” x 12” x 1/64”)
- (2) Copper Sheet (6” x 12” x 0.016”)
- (4) Tin sheet (4” x 10” x 0.013”)
- JB Weld Epoxy (Cold-Weld Steel Reinforced Solution)
- 50’ Ethernet Cable
- Calaculator

Procedures:

CONTROL GROUP:

A. Setup

1. As directed in the “QuarkNet Cosmic Ray Muon Detector (CRMD) Assembly Instructions for Series 6000 DAQ,” setup the scintillation detector on a clear surface (Appendix A.3). The location of the detector will need to remain stationary with a local wall plug to use.
2. Leave the connections to the counters unplugged and slide the support system onto the paddles. The side with the lip of the 3D support slide both longer ends of the PVC tube of each counter into the device and ensure the paddles lay parallel to each other. Slide another 3D printed support onto the opposite end of the paddles PVC pipes with the lip facing towards the scintillator.

3. Finish setting up the detector by plugging in the counters to the DAQ. Ensure that the GPS module has a connection: Green = Connected, Red = No Connection. (Note: Depending on the location of the detector from a window, GPS module need to be in the window to receive a signal. Adjust the length of the Ethernet cable as necessary.)
4. Using the PuTTY program downloaded from putty.org, open the program and select “Serial” under connection type, set the serial port to what port the detector USB is connected to, and set the speed to 115200. Under “Saved Session”, type in a title for the connection, “Save” session, and select the saved name to click the “Load” icon.
5. On the left hand side of the detector select under “Session” the “Logging” icon. Under “Session Logging”, select “All Session Output”, and unclick “Flush log Frequently”. Under Log name file, click “Browse”, and select the folder and name of file to save trial.
6. Now select the open icon at the bottom of the page. Type the command “RB” to reboot the detector, “ST 3 1” to set the counter to reset after 1 minutes, and “CE” to enable the program to record data. After a minute stop the program with the command “CD” and save the data by right clicking on the bar at the top of the program window, select “Change Setting”, select “None” under “Session Logging”, and click “Apply”.
7. Go to the site i2u2.org, select “Cosmic Ray E-Lab”, “Student Home”, and log in as a guest or with given credentials. Commit Geometry for the amount of time data is being collected for with “Stacked” orientation and time set at 5:00 UTC for each entry (Appendix A.2).
8. Select “Upload”, “Upload Raw Data”, and select the detector number, the benchmark being used (Appendix A.1), “Benchmark 1”, type in the file name to identify under

comments, and choose file to upload under "Browse" and select the "Upload" icon at the bottom of the page. If the upload provides a count without any errors proceed to next step, otherwise troubleshoot problem by checking connections to the computer and GPS.

B. Control:

1. Close the PuTTY program and reopen it to follow steps 4-6 again for the control trial. This time change the title to "Control" in step 5 and change the ST command to "ST 3 5" to reset counters after 5 minutes in step 6.
2. Record the time and allow the computer to record data for 24 hours to stop data collection as explained in step 6. Open file at saved location on computer and separate the file by every 96th "ST" line using the "Crtl+F" function to locate the command line. This divides the data in 8 hour integrals, save each 8 hour period in a separate notepad document name file as "Control" and numbered trial. There should be 3 trials per material each 8 hours long, then follow step 8 in "Setup" to upload each trial.
3. After uploading the file, a page will appear with Blessing information (Appendix A.1), event count, and any error messages. Record the channel event count per channel number and the coincidence count by selecting '"Data", "View Data", select the location, and the date of the data trial to record the count (check if correct file, by looking at comment).

EXPERIMENTAL GROUP:

Test 1: Confirm Cloud Chamber Results

1. Materials are pre-cut and sized nearest to the dimensions of the detector plate of the scintillation detector.

2. Place one of the shielding materials directly centered within the two paddles (Polyethylene, Lead, and Aluminum). *HANDLE LEAD SHEET METAL WITH SAFETY GLOVES, APRON, AND GOGGLES. WASH HANDS AFTER USE AND STORAGE*
3. Follow steps 1-3 under the control section of procedures for data recording, name document by its material and trial number when uploading.
4. Test the other two shielding materials listed in step 2 under the experimental section of procedures. Repeat listed process for data recording.

Test 2: Shielding Material Based on Density

1. For this part of the experiment the student researcher will be testing five additional materials including: Gold, Silver, Tin, Copper, and Steel. Repeating the process described in part 1.
2. Follow steps under control procedures for new materials. There should be 3 trials per material and five materials being tested in the detector.

Test 3: Effectiveness of Composite

1. Refer to the muon count average for the 8 materials and note the two top materials in reducing the event count in the scintillation detector.
2. Depending on the two effective materials, use Epoxy Weld Bonding Compound solution and apply a dot worth to each corner. Apply pressure by placing 5 to 10 textbook on top of the two most effective shields in the scintillation detector. Allow at least 10 minutes for the solution to dry between the two materials (If the two most effective shields

include Gold or Silver, place the two most effective shields flushed on top of each other rather than bonding due to fragile material).

3. Follow steps in control section of procedures to collect data following same procedures for other materials.

Data Analysis:

DATA:

Key:

t = time (hrs)
ρ = density (g/cm^3)
W = Width (cm)
1 = Channel 1 (events)
Coincidence = Coincidence Count (events)

m = mass (g)
L = Length (cm)
H = Height (cm)
2 = Channel 2 (events)

CONTROL:

Table 1:

			Channel # Count (events)		
Trial	File Name	t	1	2	Coincidence
1	6467.2017.0127.2	8	41277	364521	19879
2	6467.2017.0128.3	8	41311	364664	19989
3	6467.2017.0128.4	8	41619	366895	20260

EXPERIMENTATION:

Table 2: Test 1- Confirm Cloud Chamber Results

						Dimensions (cm)		Channel # Count (events)		
Trial	File Name	t	Material	ρ	m	L	W	1	2	Coincidence
1	6467.2017.0208.1	8	Polyethylene	0.94	66.1	30.48	30.48	41718	364762	20539
2	6467.2017.0208.2 6467.2017.0209.0	8	Polyethylene	0.94	66.1	30.48	30.48	41055	360346	20262
3	6467.2017.0209.1	8	Polyethylene	0.94	66.1	30.48	30.48	40984	361366	20136
1	6467.2017.0206.0	8	Aluminum	2.7	2.8	31.12	25.72	41589	365191	20311
2	6467.2017.0207.0	8	Aluminum	2.7	2.8	31.12	25.72	41467	367061	20169
3	6467.2017.0207.1 6467.2017.0208.0	8	Aluminum	2.7	2.8	31.12	25.72	42016	367127	20585
1	6467.2017.0209.2 6467.2017.0210.0	8	Lead	11.35	406.8	30.48	30.48	43629	369185	21049
2	6467.2017.0210.1	8	Lead	11.35	406.8	30.48	30.48	43764	365270	21072
3	6467.2017.0210.2	8	Lead	11.35	406.8	30.48	30.48	42477	360349	20335

Table 3: Test 2- Shielding Materials Based on Density

						Dimensions (cm)		Channel # Count (events)		
Trial	File Name	t	Material	ρ	m	L	W	1	2	Coincidence
1	6467.2017.0131.2	8	Tin	7.29	209.8	30.48	25.4	42005	364654	20124
2	6467.2017.0131.3 6467.2017.0201.0	8	Tin	7.29	209.8	30.48	25.4	42436	365559	20298
3	6467.2017.0201.1	8	Tin	7.29	209.8	30.48	25.4	42476	366705	20342
1	6467.2017.0130.2	8	Steel	7.85	603.2	45.72	30.48	43379	367228	20629
2	6467.2017.0130.3 6467.2017.0131.0	8	Steel	7.85	603.2	45.72	30.48	42971	365424	20359
3	6467.2017.0131.1	8	Steel	7.85	603.2	45.72	30.48	42506	366240	20265
1	6467.2017.0201.2 6467.2017.0202.0	8	Copper	8.96	337.2	30.48	30.48	42857	362967	20315
2	6467.2017.0202.1	8	Copper	8.96	337.2	30.48	30.48	42616	364828	20643
3	6467.2017.0202.2	8	Copper	8.96	337.2	30.48	30.48	42987	364462	20749
1	6467.2017.0202.3 6467.2017.0203.0	8	Silver	10.5	1	31.12	25.72	41454	364083	20376
2	6467.2017.0203.1	8	Silver	10.5	1	31.12	25.72	41455	363075	20250
3	6467.2017.0203.2	8	Silver	10.5	1	31.12	25.72	40983	364018	20183
1	6467.2017.0203.3 6467.2017.0204.0	8	Gold	19.3	0.8	31.12	25.72	41195	360304	20076
2	6467.2017.0204.1	8	Gold	19.3	0.8	31.12	25.72	41113	360724	20268
3	6467.2017.0204.2	8	Gold	19.3	0.8	31.12	25.72	40765	361329	19880

Table 4: Test 3- Effectiveness of Composite Material

						Channel # Count (events)		
Trial	File Name	t	Material	ρ	m	1	2	Coincidence
1	6467.2017.0211.0	8	Gold-Tin	7.34	210.6	41103	364294	20501
2	6467.2017.0211.1	8	Gold-Tin	7.34	210.6	41391	363649	20560
3	6467.2017.0211.2 6467.2017.0212.0	8	Gold-Tin	7.34	210.6	41539	367571	20691

RESULTS:

Key:

CAvg = Coincidence Count Average (events)

A = Area (cm^2)

I = Event Count

I_o = Initial Event Count

V = Volume

μ = Area/Mass (cm^2/g)

α = Linear Attenuation Coefficient

% = Percent Difference

x = Thickness (cm)

Table 5: Test 1- Confirm Cloud Chamber Results

Material	CAvg	I_o	V	A	μ	α	x	I	%
Polyethylene	20312	20043	70.32	929.03	14.05	13.21	0.076	7343	93.79
Aluminum	20355	20043	1.04	800.41	285.86	771.82	0.0013	7349	93.90
Lead	20819	20043	35.84	929.03	2.28	25.92	0.039	7293	96.22

Table 6: Test 2- Shielding Materials Based on Density

Material	CAvg	I_o	V	A	μ	α	x	I	%
Tin	20255	20043	28.78	774.19	3.69	26.90	0.037	7408	92.88
Steel	20418	20043	76.84	1393.55	2.31	18.14	0.055	7392	93.67
Copper	20569	20043	37.63	929.03	2.76	24.69	0.041	7285	95.39
Silver	20270	20043	0.095	800.41	800.41	8404.27	0.00012	7373	93.31
Gold	20075	20043	0.041	800.41	1000.51	19309.80	0.000052	7372	92.57

Table 7: Test 3- Effectiveness of Composite Material

Material	CAvg	I_o	V	A	μ	ρ	α	I	%
Gold-Tin	20584	20043	28.68	774.19	3.68	7.34	26.98	7375	94.49

From the collected data, the most effective shield was gold with a average coincidence count of 20075 events followed by Tin with a count of 20255 events. This average was calculated by adding the coincidence count of each trial that was 8 hours long and dividing by the number of trials. Since gold and tin had the lowest event count, the two were placed in the detector with an averaged count of 20584 events. To compare results to the accepted count per material, with consideration to thickness and density of material, Lambert's law equation for linear attenuation of radiation was used to calculate the accepted value for each material with the equation $I = I_o e^{-\alpha x}$ to figure out the amount of particles that passed through each material. Gold had a coincidence count of 7372 events and tin with 7408 events for the calculated particle count. To illustrate the difference between the experimental and calculated value, percent difference was figured for each material. Gold-tin had a 94.49% difference between the average 20584 and calculated 7375 events, gold with 92.57%, and tin with 92.88%.

Graph 1: Control Coincidence Count

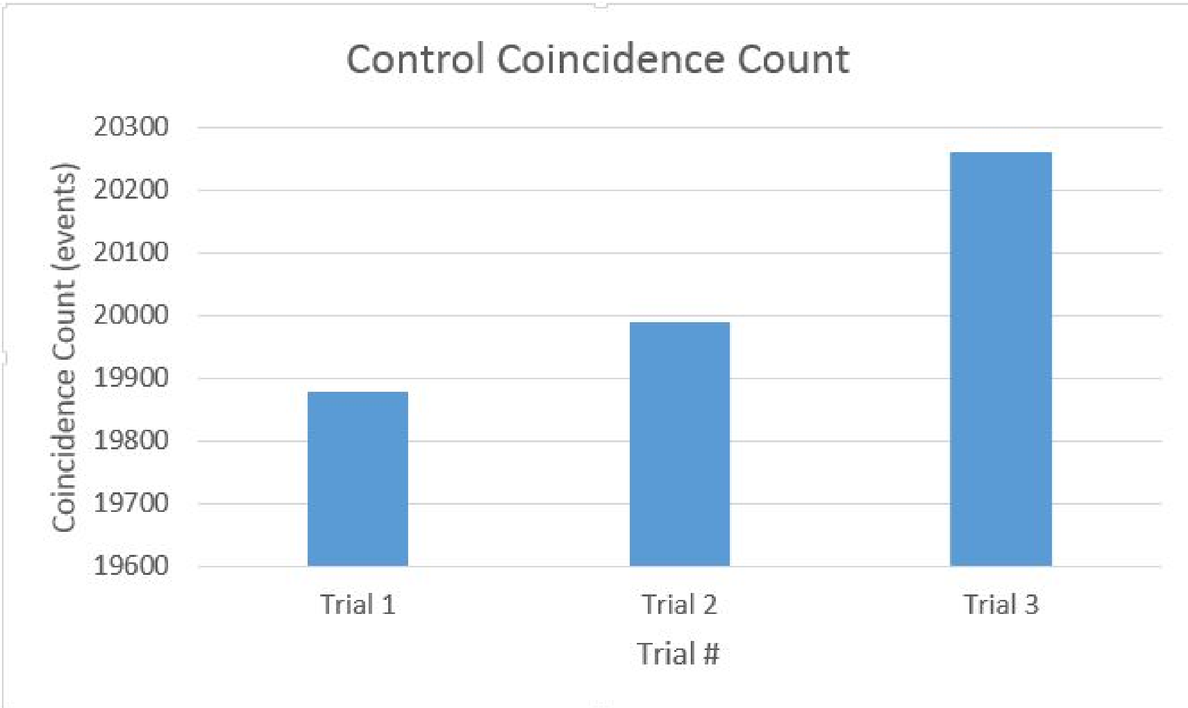

Graph 2: Test 1 Coincidence Count Based on Material

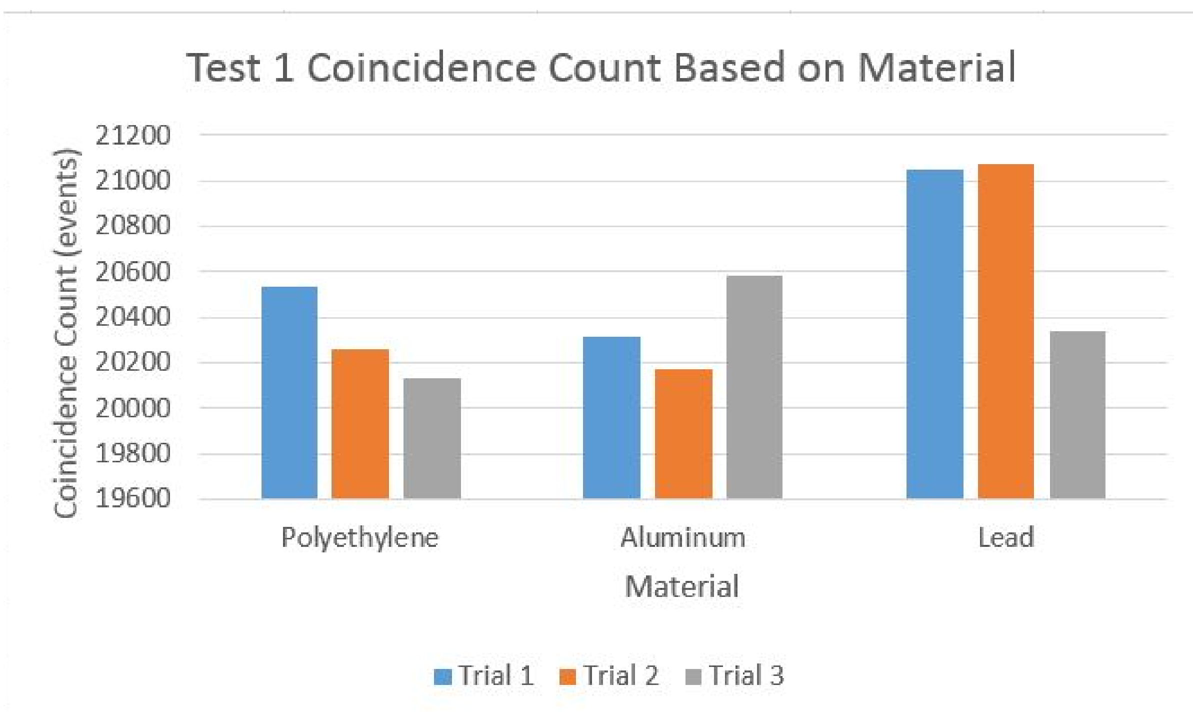

Graph 3: Test 2 Coincidence Count Based on Material

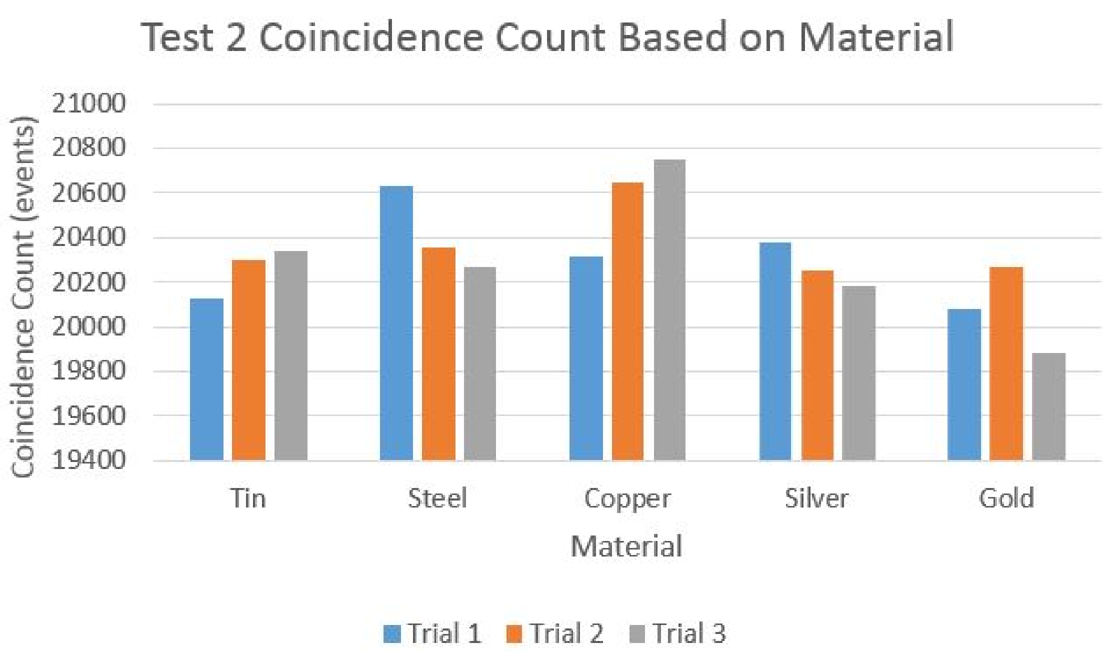

Graph 4: Gold-Tin Coincidence Count

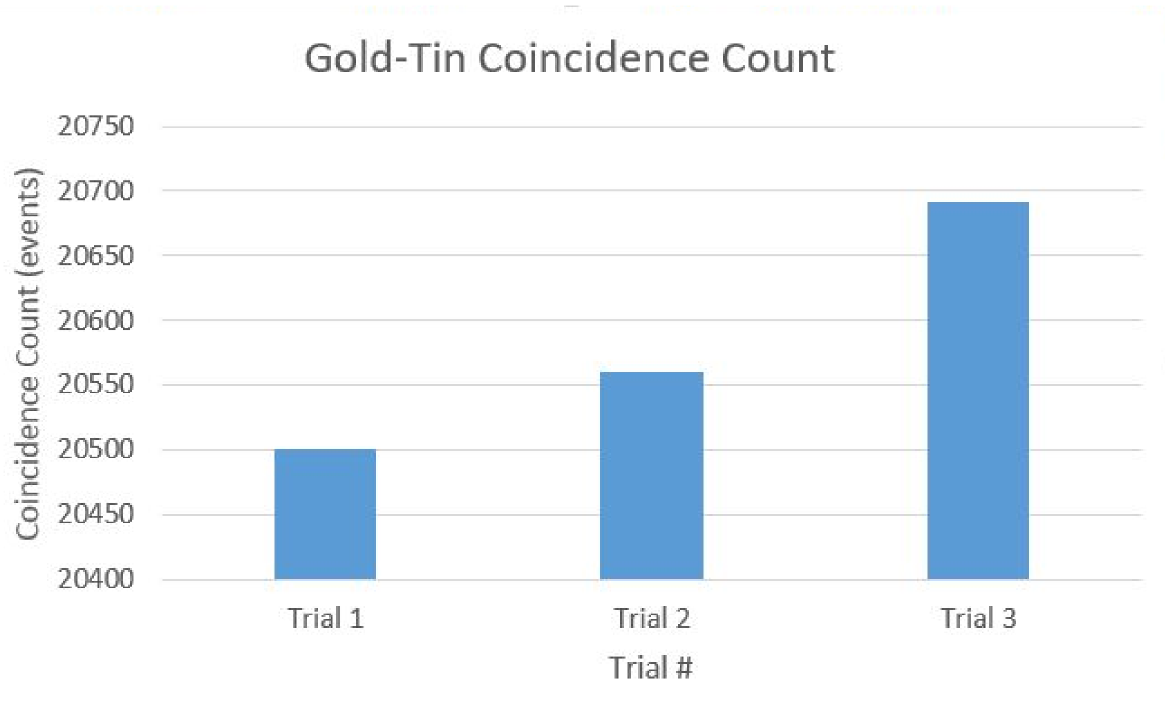

Graph 5: Coincidence Count Based on Material

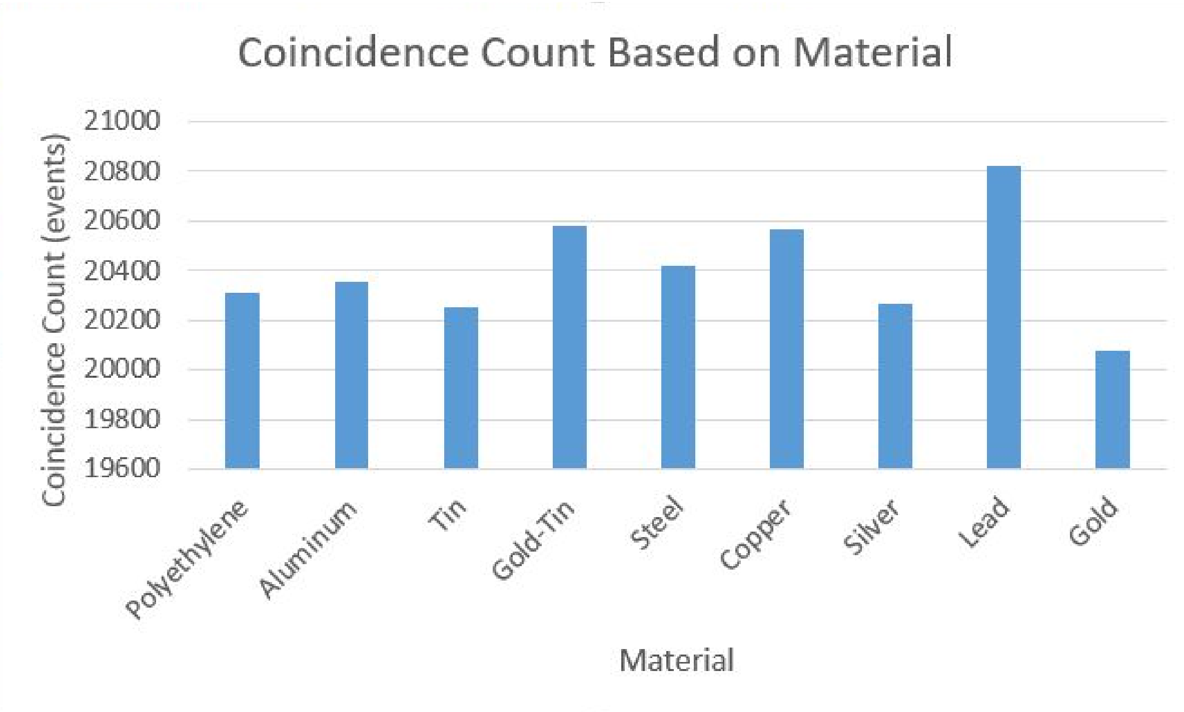

Graph 6: Coincidence Count Based on Density

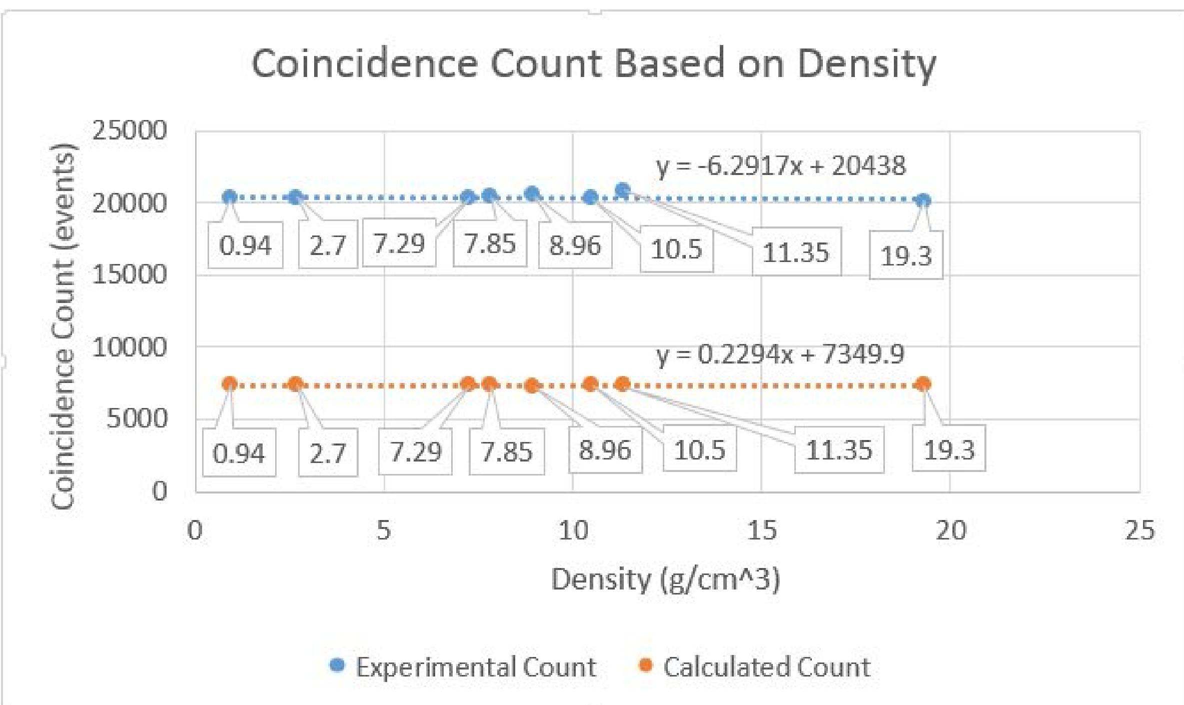

Separating the tests by each material and the control, allows the researcher to analyze each trial individually; however graph 5 shows the overall effectiveness of each material illustrating that gold had the lowest count with 20075 events and lead with the highest count at 20819 events. Graph 6 shows how varying density of the material alters the muon count in the line graph above. The text boxes near each data point represents the density of the material and corresponds to graph 5 materials from left to right.With both the experimental and calculated densities displayed, the trendline for experimental count showed a decrease in event count with increase in density of a material given the equation of the line to be y = -6.2917x + 20413 and a decreasing slope of -6.2917 events by increasing the density by 1 g/cm^3.

STATISTICAL ANALYSIS:

Table A:

Control	Flux (events/(s)(m^2)	Mean	Standard Deviation	Z-score	Area Under the Curve	Probability (%)
1	513	520	6	-1.22	0.1112	11.12
2	514	520	6	-1.00	0.1587	15.87
3	517	520	6	-0.50	0.3085	30.85
4	517	520	6	-0.50	0.3085	30.85
5	520	520	6	0.00	0.5000	50.00
6	520	520	6	0.00	0.5000	50.00
7	522	520	6	0.33	0.6293	37.07
8	526	520	6	1.00	0.8413	15.87
9	531	520	6	1.83	0.9664	3.36

Table B:

Polyethylene	Flux (events/(s)(m^2)	Mean	Standard Deviation	Z-score	Area Under the Curve	Probability (%)
1	517	528	7	-1.51	0.0582	5.82
2	521	528	7	-1.00	0.1587	15.87
3	525	528	7	-0.43	0.3336	33.36
4	526	528	7	-0.29	0.3859	38.59
5	526	528	7	-0.29	0.3859	38.59
6	527	528	7	-0.14	0.4443	44.43
7	531	528	7	0.43	0.6628	57.14
8	537	528	7	1.29	0.9015	9.85
9	538	528	7	1.43	0.9357	6.43

Table C:

Aluminum	Flux (events/(s)(m^2)	Mean	Standard Deviation	Z-score	Area Under the Curve	Probability (%)
1	513	529	9	-1.81	0.0351	3.51
2	522	529	9	-0.78	0.2177	21.77
3	523	529	9	-0.67	0.2514	25.14
4	527	529	9	-0.22	0.4129	41.29
5	528	529	9	-0.11	0.4562	45.62
6	535	529	9	0.67	0.7486	25.14
7	535	529	9	0.67	0.7486	25.14
8	537	529	9	0.89	0.8133	18.67
9	541	529	9	1.33	0.9082	9.18

Table D:

Lead	Flux (events/ (s)(m^2)	Mean	Standard Deviation	Z-score	Area Under the Curve	Probability (%)
1	527	542	9	-1.68	0.0465	4.65
2	536	542	9	-0.67	0.2514	25.14
3	536	542	9	-0.67	0.2514	25.14
4	538	542	9	-0.44	0.3300	33.00
5	542	542	9	0.00	0.5000	50.00
6	544	542	9	0.22	0.5871	41.29
7	550	542	9	0.89	0.8133	18.67
8	553	542	9	1.22	0.8888	11.12
9	555	542	9	1.44	0.9251	7.49

Table E:

Tin	Flux (events/ (s)(m^2)	Mean	Standard Deviation	Z-score	Area Under the Curve	Probability (%)
1	514	525	5	-2.33	0.0099	0.99
2	524	525	5	-0.20	0.4207	42.07
3	525	525	5	0.00	0.5000	50.00
4	526	525	5	0.20	0.5793	42.07
5	527	525	5	0.40	0.6554	34.46
6	527	525	5	0.40	0.6554	34.46
7	528	525	5	0.60	0.7257	27.43
8	529	525	5	0.80	0.7881	21.19

Table F:

Steel	Flux (events/ (s)(m^2)	Mean	Standard Deviation	Z-score	Area Under the Curve	Probability (%)
1	525	530	6	-0.87	0.1922	19.22
2	525	530	6	-0.83	0.2033	20.33
3	527	530	6	-0.50	0.3085	30.85
4	528	530	6	-0.33	0.3707	37.07
5	528	530	6	-0.33	0.3707	37.07
6	528	530	6	-0.33	0.3707	37.07
7	531	530	6	0.17	0.5675	43.25
8	537	530	6	1.17	0.8790	12.10
9	543	530	6	2.17	0.9850	1.50

Table G:

Copper	Flux (events/ (s)(m^2)	Mean	Standard Deviation	Z-score	Area Under the Curve	Probability (%)
1	523	534	6	-1.74	0.0409	4.09
2	526	534	6	-1.33	0.0918	9.18
3	533	534	6	-0.17	0.4325	43.25
4	534	534	6	0.00	0.5000	50.00
5	534	534	6	0.00	0.5000	50.00
6	536	534	6	0.33	0.6293	37.07
7	537	534	6	0.50	0.6915	30.85
8	542	534	6	1.33	0.9082	9.18
9	542	534	6	1.33	0.9082	9.18

Table H:

Silver	Flux (events/ (s)(m^2)	Mean	Standard Deviation	Z-score	Area Under the Curve	Probability (%)
1	514	526	6	-1.97	0.0244	2.44
2	523	526	6	-0.50	0.3085	30.85
3	523	526	6	-0.50	0.3085	30.85
4	526	526	6	0.00	0.5000	50.00
5	527	526	6	0.17	0.5675	43.25
6	528	526	6	0.33	0.6293	37.07
7	529	526	6	0.50	0.6915	30.85
8	530	526	6	0.67	0.7486	25.14
9	537	526	6	1.83	0.9664	3.36

Table I:

Gold	Flux (events/ (s)(m^2)	Mean	Standard Deviation	Z-score	Area Under the Curve	Probability (%)
1	516	522	4	-1.34	0.0901	9.01
2	517	522	4	-1.25	0.1056	10.56
3	518	522	4	-1.00	0.1587	15.87
4	520	522	4	-0.50	0.3085	30.85
5	521	522	4	-0.25	0.4013	40.13
6	523	522	4	0.25	0.5987	40.13
7	526	522	4	1.00	0.8413	15.87
8	526	522	4	1.00	0.8413	15.87
9	527	522	4	1.25	0.8944	10.56

Table J:

Gold-Tin	Flux (events/(s)(m^2)	Mean	Standard Deviation	Z-score	Area Under the Curve	Probability (%)
1	524	535	6	-1.87	0.0307	3.07
2	530	535	6	-0.83	0.2033	20.33
3	532	535	6	-0.50	0.3085	30.85
4	534	535	6	-0.17	0.4325	43.25
5	535	535	6	0.00	0.5000	50.00
6	536	535	6	0.17	0.5675	43.25
7	536	535	6	0.17	0.5675	43.25
8	541	535	6	1.00	0.8413	15.87
9	543	535	6	1.33	0.9082	9.18

Graph A:

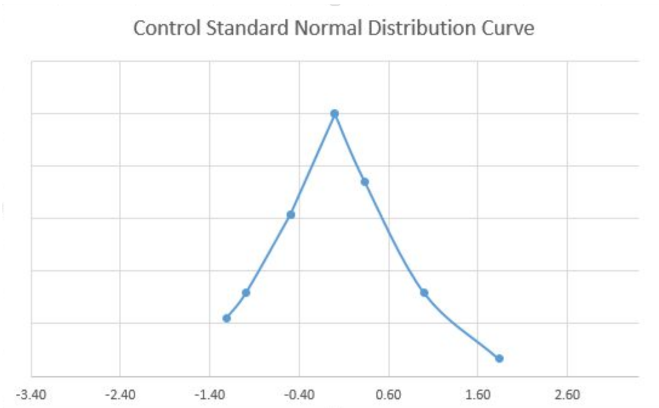

Graph B:

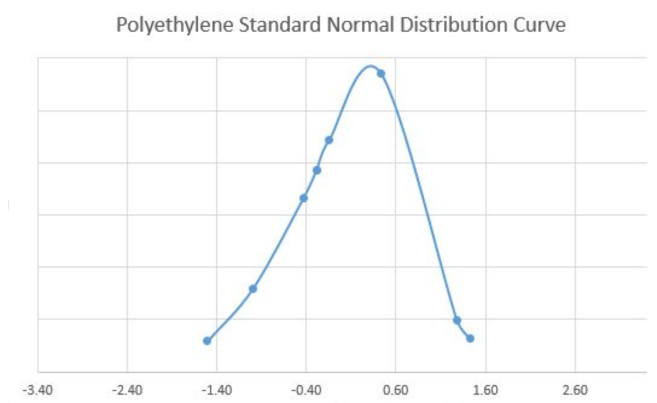

Graph C:

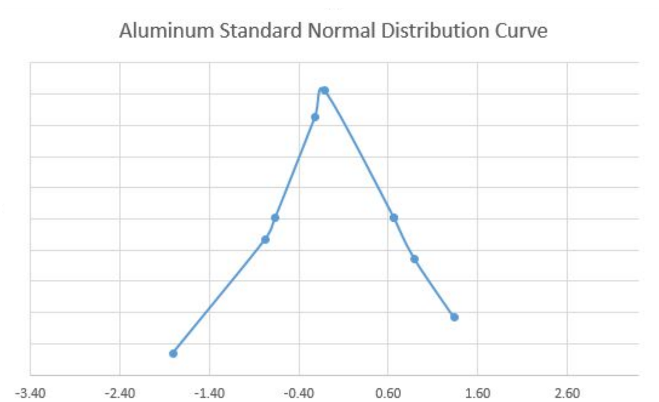

Graph D:

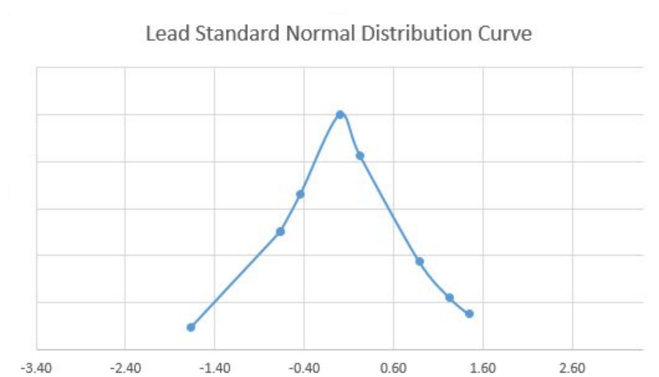

Graph E:

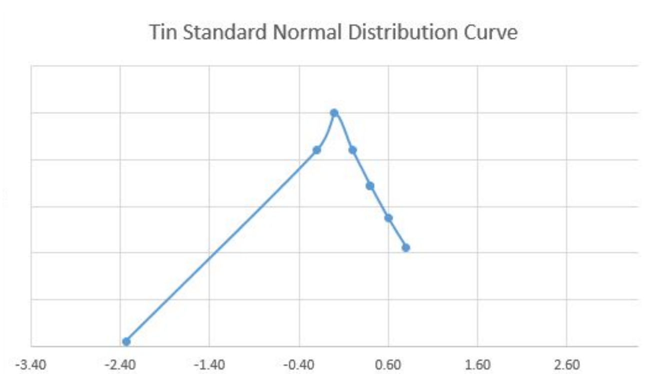

Graph F:

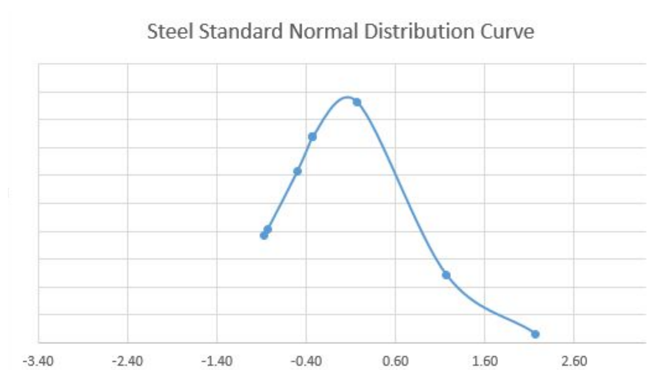

Graph G:

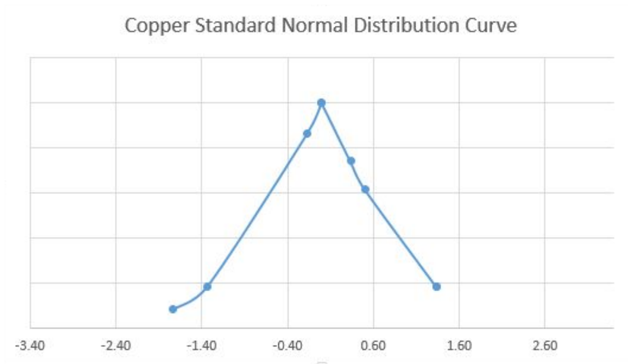

Graph H:

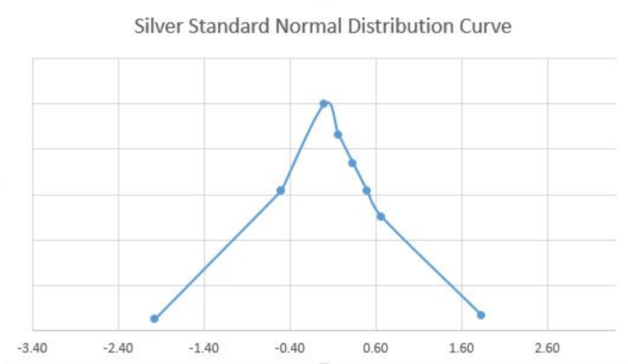

Graph I:

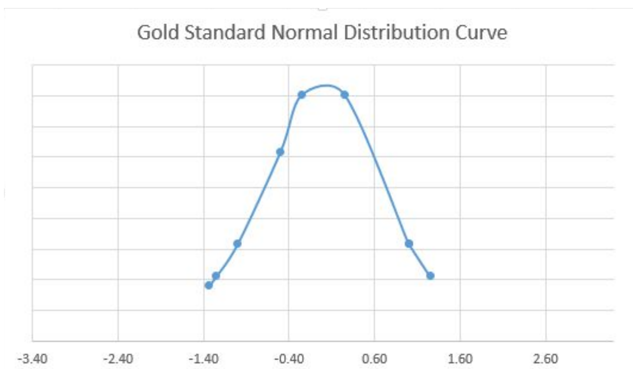

Graph J:

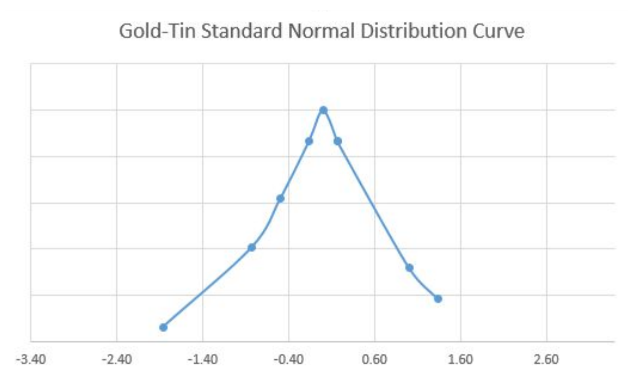

The statistical analysis section looked to ensure that the data received by the detector reflected the effects of the independent variable and not the environment. The student researcher used the flux studies feature from the "Cosmic Ray E-Lab" site to find the sample data set of each material. Three bins were created by changing the bin width to 9600 s or 160 minutes to receive 3 data points per material trial. With 9 data points, the z-score was calculated by figuring the standard deviation and the mean of the sample using the equations as explained in the "Sample Calculations" examples 7, 8, and 9. After the z-score was found, one can plot the Standard Normal Distribution Curve using the Area under the Curve Chart to figure the probability of each data point on the graph ("Sample Calculations" Example 10). As depicted above, each test was created a Standard Normal Distribution Curve following a upside down "V" or "U" shape resembling the Bell Curve. Variation in shape is evident between Copper and Gold for example; however the bell-like shape suggests that the trials throughout the month was unaffected by outside factors such as rain, snow, or lighting in the environment as well as solar activity from the sun.

SAMPLE CALCULATIONS:

Example 1-

What is the average coincidence count of the control trial given that trial 1, 2, and 3 counts were 19879, 19989, and 20260 events?

Average Coincidence Count = (Trial 1 + Trial 2 + Trial 3) / 3

CAvg = (Trial 1 + Trial 2 +Trial 3) / 3

CAvg = (19879 events + 19989 events + 20260 events) / 3

<u>CAvg = 20042.67 events ≈ 20043 events</u>

Example 2-

What is the volume of the polyethylene sheet given the mass to be 66.1 g and the density to be 0.94 g/cm^3?

Density = mass/ volume

ρ = m/V

V = m/ρ

V = 66.1 g/ 0.94 g/cm^3

<u>V = 70.32 cm^3</u>

Example 3-

What is the Area of the polyethylene sheet given the length x width to be 30.48 cm x 30.48 cm?

Area = Length x Width

A = L x W

A = (30.48 cm)(30.48 cm)

$\underline{A = 929.03\ cm^2}$

Example 4-

What is the thickness of the polyethylene sheet given its Volume and Area to be 70.32 cm^3 and 929.03 cm^2 respectively?

Volume = Length x Width x Height

Area = Length x Width

Volume = Area x Height

V = (A)(x)

x = V/A

x = 70.32 cm^3 / 929.03 cm^2

$\underline{x = 0.076\ cm}$

Example 5-

What is the calculated Event count from the polyethylene sheet given the initial count as 20043 events, thickness to be 0.076 cm, the density is 0.94 g/cm^3, Area is 929.03 cm^2, and the mass of the material is 66.1 grams?

$\text{Event Count} = (\text{Initial Count})e^{-[(\text{Area/mass})(\text{Density})](\text{Thickness})}$

$I = I_o e^{-\alpha x}$

$I = I_o e^{-(\mu\rho)x}$

$I = (20043\ \text{events})e^{-[(929.03\ cm\wedge 2\ /\ 66.1\ g)(0.94\ g/cm\wedge 3)](0.076\ cm)}$

$I = (20043\ \text{events})e^{-(13.21\ cm\wedge\text{-}1)(0.076\ cm)}$

$I = (20043\ \text{events})e^{-1.004}$

I = (20043 events)(0.37)

$\underline{I = 7343.36\ \text{events} \approx 7343\ \text{events}}$

Example 6-

What is the percent difference between the experimental recorded event count versus the calculated count with values 20312 and 7343 events?

Percent Difference (%) =[|Experimental - Calculated| / ((Experimental + Calculated)/2)] x 100

% = [|20312 events - 7343 events| / ((20312 events + 7343 events)/2)] x 100

% = (12969 / 13827.5) x 100

<u>% = 93.79 %</u>

Example 7-

What is the mean of the nine data points from the sample data set in flux study of the control trials: 513, 514, 517, 517, 520, 520, 522, 526, and 531 events/ (s)(m^2)?

Mean = Total data point value of sample data set/ number of data points

$\mu = (x_1 + x_2 + x_3 + \ldots)/ n$

$\mu = (513 + 514 + 517 + 517 + 520 + 520 + 522 + 526 + 531) / 9$

<u>μ = 520 events/ (s)(m^2)</u>

Example 8-

What is the standard deviation of the sample data set above in example 7?

Standard Deviation = √Sum of (Data point- Mean of sample data set)^2 / (number of data points - 1)

$\sigma = \sqrt{} \Sigma(x - \mu)^2 / n-1$

$\sigma = \sqrt{} [(513 - 520)^2 + (514 - 520)^2 + (517 - 520)^2 + (517 - 520)^2 + (520 - 520)^2 +(520 - 520)^2 + (522 - 520)^2 + (526 - 520)^2 +(531 - 520)^2] / (9-1)$

<u>σ = 6 events/ (s)(m^2)</u>

Example 9-

What is the z-score of the 513 events/(s)(m^2), if the standard deviation is 6 units and the mean of the data is 520 events/(s)(m^2)?

Z-score = (Data point - mean)/ Standard deviation

$z = (x - \mu)/ \sigma$

$z = (513 - 520)/ 6$

<u>z = -1.17</u>

Example 10-

What is the probability percentile on the standard normal distribution curve for this data point?

z = -1.17 ---> Standard Normal Distribution Curve Area chart ---> A= 0.1210

z = + # ---> (1- Area) x 100 = Probability %

z = - # ---> Area x 100 = Probability %

Probability = 0.1210 x 100

Probability = 12.10%

Conclusion:

Gold and tin were the most effective materials in the scintillation detector, rejecting the original hypothesis that samples of gold and silver would be the two most effective materials due to their higher densities compared to the other tested materials. Gold had the lowest experimental coincidence count with 20075 events since it had a high density of 19.3 g/cm^3 and tin had a count of 20255 events although it had a density of 7.29 g/cm^3 and its thickness was 0.037 cm. When the two material were placed on top of each other as the "Composite Material," the count was recorded as 20584 events since the calculated density of the composite was 7.34 g/cm^3. The results of this experiment can be due to errors in data collection which lead to the percent difference of 90% or greater. The percent difference cannot be accounted for by variations in the system, because of the z-score calculations and plotted Standard Normal Distribution Curves using the data from the Flux Study feature on the "Cosmic Ray E-Lab" site. After figuring the z-score, the Area under the curve could be found in the Standard Normal Distribution Curve Table used to figure the probability percentile of each data point. All tests reflected the bell curve shape, demonstrating that the data collected was unaffected by changes in time of day or seasons in relation to the effects of the sun. This analysis proves that the "muons" detected was not influenced by changes the sun's activity. However, density wasn't the only factor that affected the muon count; since thickness and density are considered in Lambert's Law, variation exist because the thickness of each material was not the same. Finding gold and silver in the same thickness of lead or copper isn't accessible at this stage, given the price and supply of such materials. Since the thickness varied, the volume also varied, and so the density wasn't the only factor affecting the final event count. To reduce variance in future experimentation, the student researcher should choose materials that are more common and can be sized at the same thickness to keep the dimensions consistence. Another area to improve is the placement of the material, since each paddle is recording any signal it receives from: muons, alpha particles, electrons, or any other charged particles. The material placed in the detector could potentially cause incoming muons to decay into smaller mass particles such as the electron, offsetting the event count when placed between the two paddles. This was evident in how the average count of events for lead, with a density of 11.35 g/cm^3 and a thickness of 0.039 cm compared to gold with 19.3 g/cm^3 and a thickness of 5.18×10^{-5} cm, was the largest event count of 20819 muons compared to the other materials. This occurrence questions if the placement allowed more secondary particles to be produced from the interaction with lead to be received by the second paddle. To improve the amount of particles received at the end of the trial, the researcher could place the material above the two paddles and compare counts from the two different orientations. Considering these limitations, there is a correlation between the density of a material and amount of particles absorbed, decayed, or reflected from each shielding material as evident by the slope of the line for the density versus coincidence count at -6.2917 events/ (1 g/cm^3). This trendline implies as the density increases, the shielding effectiveness against incoming particles is directly proportional. However, an improved shielding material was not possible for the student research to produce in this experiment because density is not additive. Density of two materials depends on the total mass of the system divided by its volume of both materials. Although gold had a density of 19.3 g/cm^3 and tin at 7.29 g/cm^3, the total mass of gold and tin is 210.6 g and volume at 28.68 cm^3 producing a density of 7.34 g/cm^3. Since the density of the composite material was reduced, the amount of particles that passed through the material was 20584 events and accepted count of 7375 events compared to gold with 20075 events and a calculated count of 7372 events. This experiment proves that layering materials without taking into consideration total volume and mass, won't produce a material with a higher density or lower event count for applications in future space related endeavors. However, it should be recognized that with the setup of this experiment, materials such as lead was effective in creating more secondary particles that may be less harmful than the primary Cosmic Rays at a higher elevation in the atmosphere. If lead was effective in turning Hydrogen nuclei or iron ions to less energetic particles such as muons in the upper atmosphere or space; suggests that instead of absorbing the particles, enough shielding should be used to slow down their speed and energy to a form that is harmless to humans or electronic systems by the time it reaches them.

Appendix:

A. PROGRAM SETUP PROCEDURES:

A.1 Geometry-

1. Login into i2u2.org site and navigate to the Cosmic Ray E-Lab site.
2. Select Geometry under the Upload link on the Cosmic Ray E-Lab home site.
3. On the left side of the page select the "Add a new entry for a detector" under the detector being used.
4. Changed the date to time that the researcher wants the detector to register setup of the detector's data.
5. Activate the number of channels used, and type in the values for the cable length, the area of each paddles and its coordinates from the GPS signal.
6. Select "Stacked" orientation for the paddles data to be recognized as having the used channels placed on top of each other.
7. Go to Google Maps and type in the address the detectors are located. Left click the mouse for a few seconds on the location and copy the coordinates into the "GPS Coordinates" section of the Geometry page. (Ensure they are in the correct format).
8. Use an altimeter or an app on a smart device and measure the altitude of the detector to record into the "Altitude" Section. Also type in the length of the GPS cable length.
9. Once information has been added to page, select "Commit Geometry" to update how the program views the orientation of the detector for data collection. Add a new entry for every day the detector is used in this orientation or is changed for data upload accuracy.

A.2 Benchmark-

1. To ensure the data is blessed or is accurate compared to the baseline or control data collected, a benchmark must be set.
2. Go to “Benchmark” under the “Upload” link on the Cosmic Ray e-Lab site.
3. Select the detector number the device used has and click the “Select Benchmark” icon on the right of the page.
4. Once the window has opened, select the control file uploaded as the control for the experiment from the list of files on the left side of the page.
5. At the bottom of the page, type in the benchmark title to be recognized as when selected later for data upload. Then save the selected benchmark. Whenever data is uploaded under this benchmark saved, the data being uploaded will be compared to the baseline to see if it should be blessed or accurate compared to set benchmark.

A.3 Detector Hardware Setup

This section deals with the assemble of the Scintillation Detector also known as Quarknet Cosmic Ray Muon Detector. This section is to distinguish that the procedures are not created by the researcher and rather was used as a reference to assemble the detector for later testing procedures. Use the link from the citation located in the “References” under Dr. Mark Adam and “Quarknet Cosmic Ray Muon Detector (CRMD) Assembly Instructions for Series 6000 DAQ” (Adams, 2012).

B. PHOTOGRAPHS AND DIAGRAMS

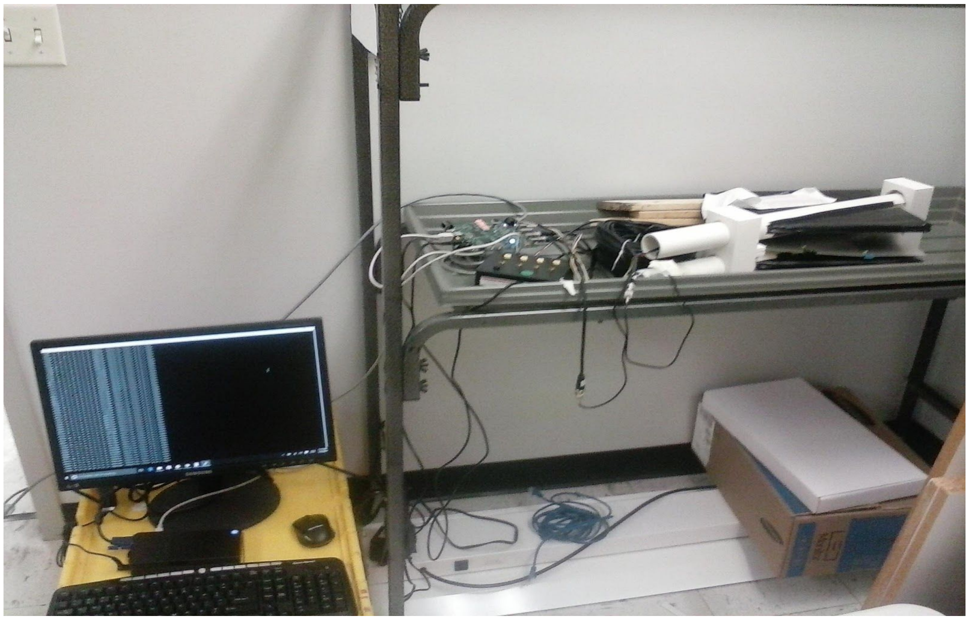

Image 1: Setup of Detector System with Computer and Paddles

Image 2: Detector Paddles with Components setup

Image 3: Detector paddles with Scintillators and Photomultiplier tubes

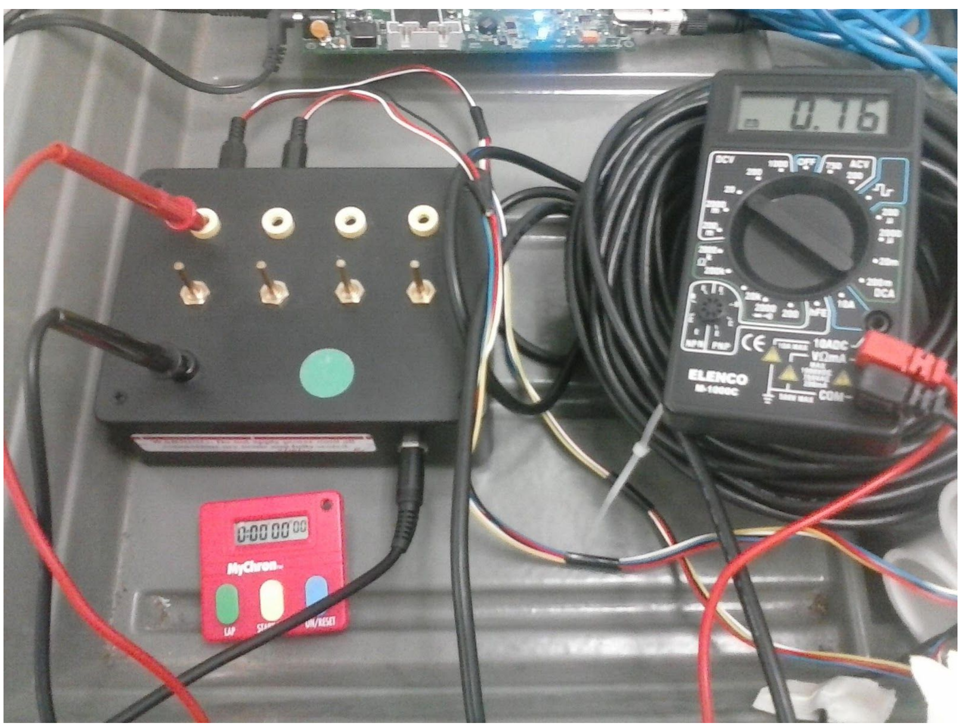

Image 4: Power Distribution Unit (PDU) depicted as plateauing is being conducted on channel 1

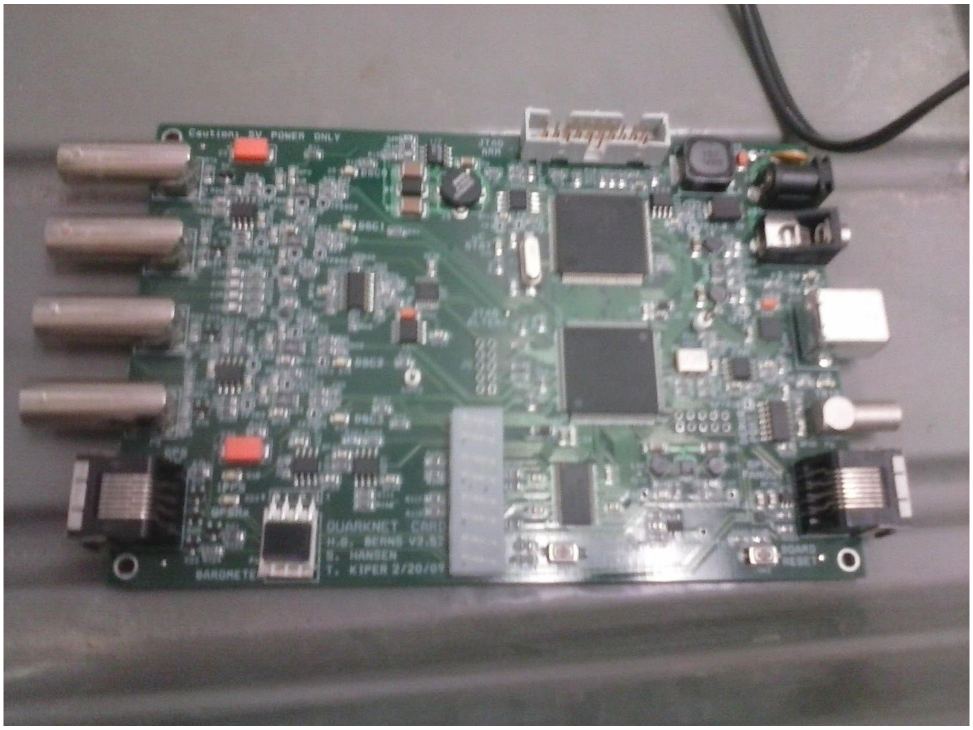

Image 5: Digital Acquisition Board (DAQ)

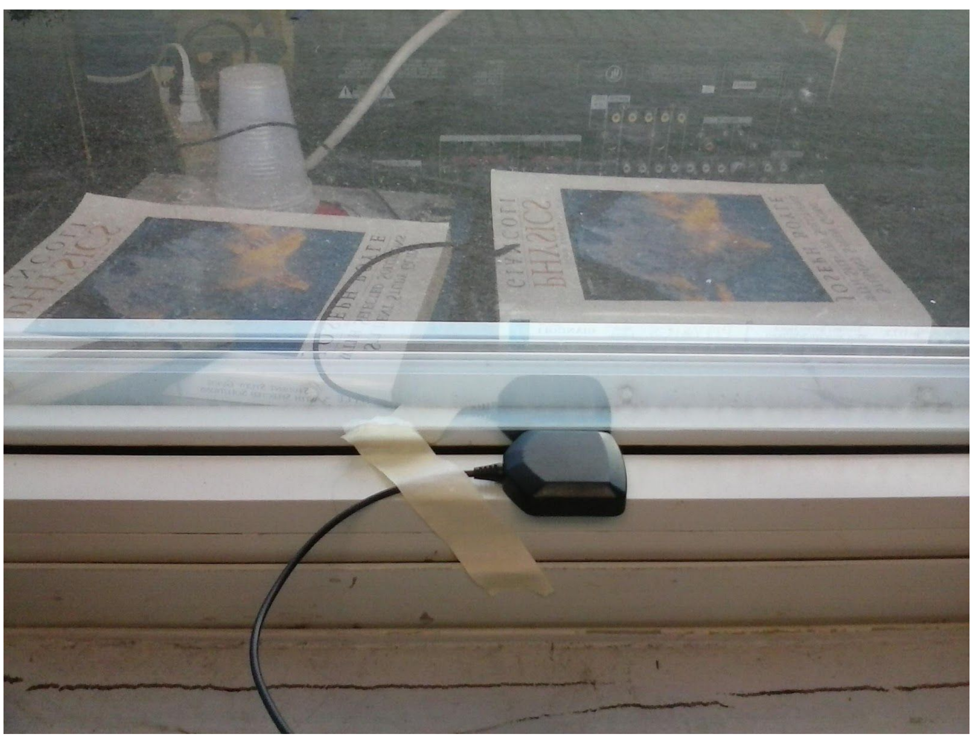

Image 6: GPS Receiver placed at window sill to receive signal from satellites

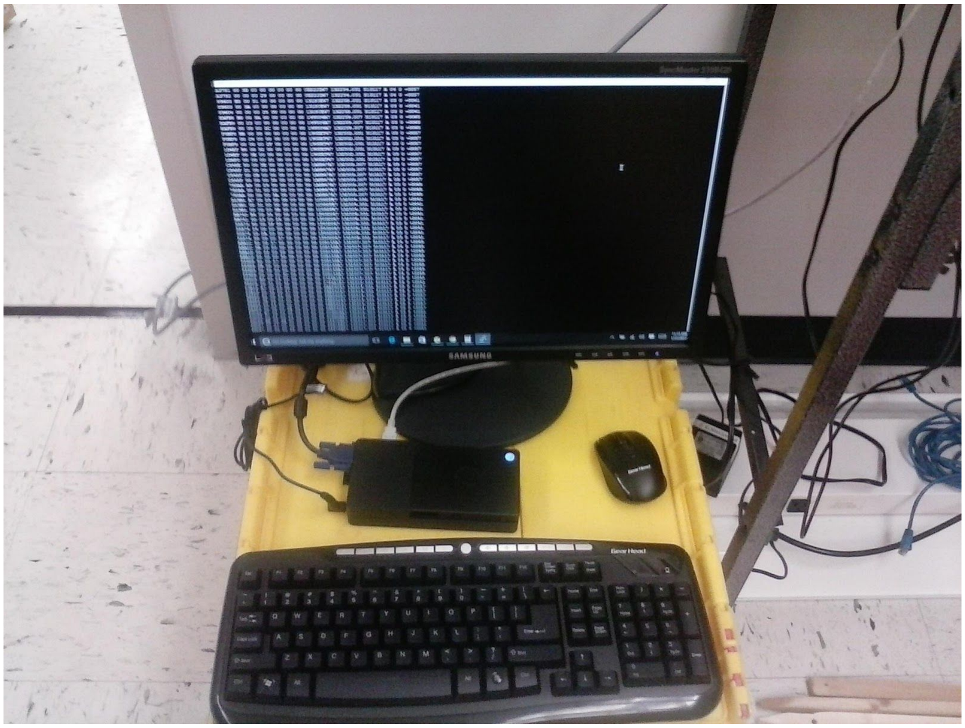

Image 7: Computer setup to receive data sent from detector

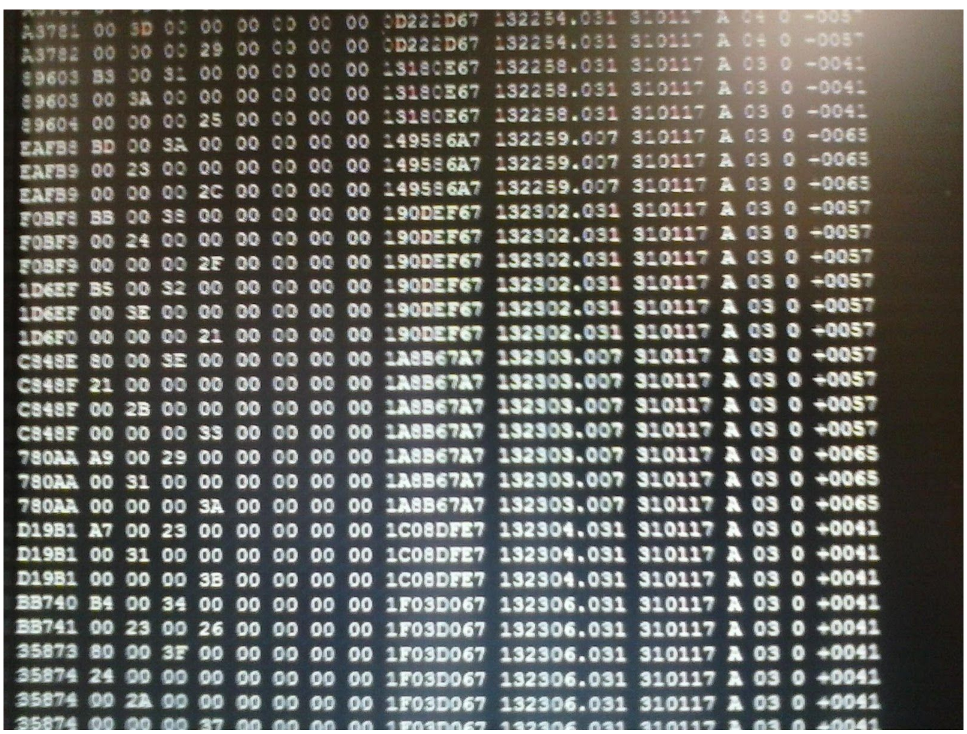

Image 8: Data displayed on Computer monitor

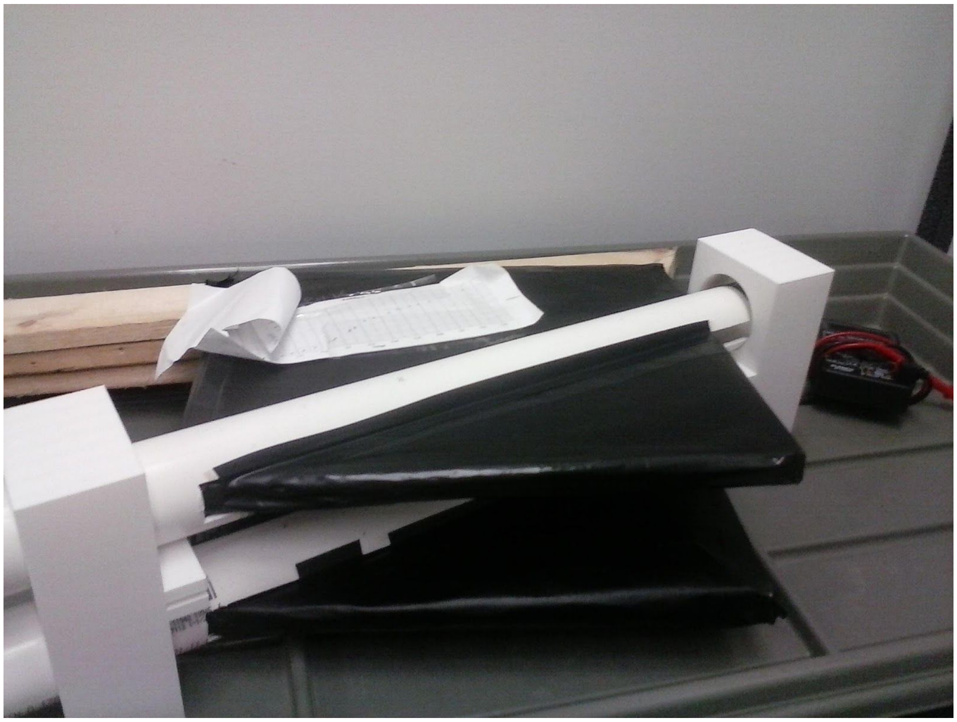

Image 9: Detector Setup without material present or control of experiment

Image 10: Polyethylene sheet

Image 11:

Aluminum Sheet

Image 12: Lead

sheet

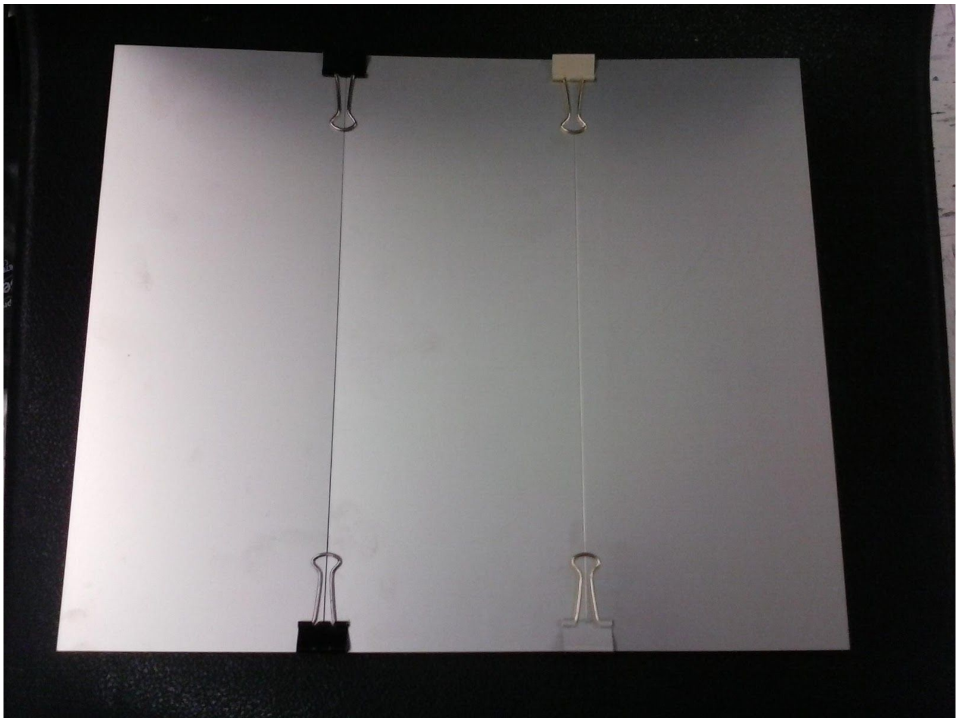

Image 13: Tin Sheet held together with binder clips

Image 14: Steel sheet

Image 15: Copper sheet

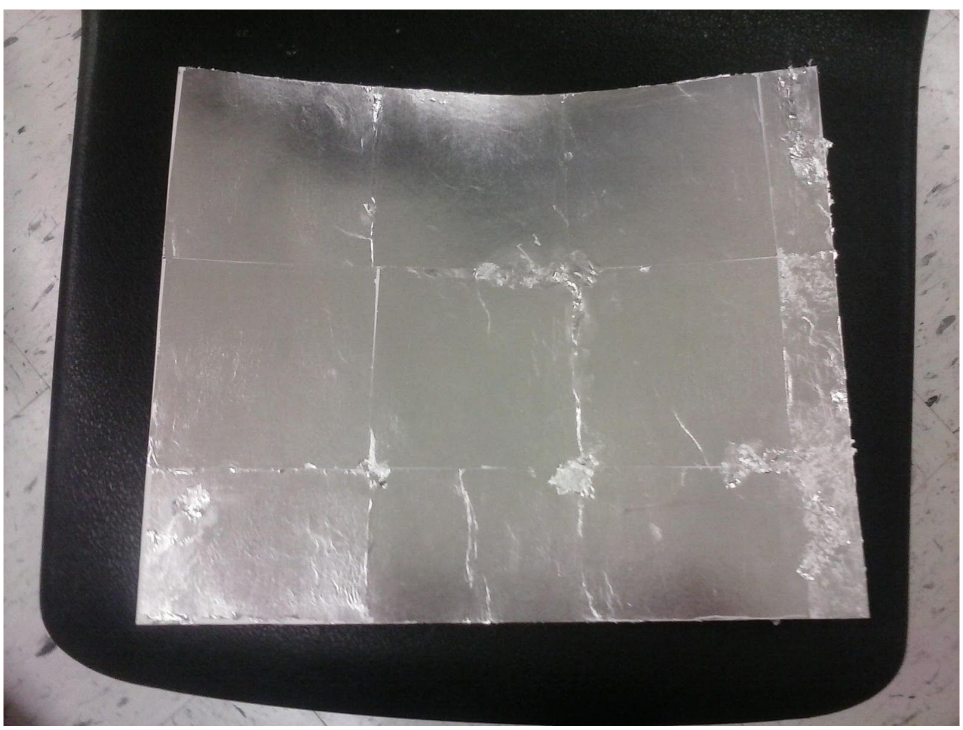

Image 16: Silver sheet

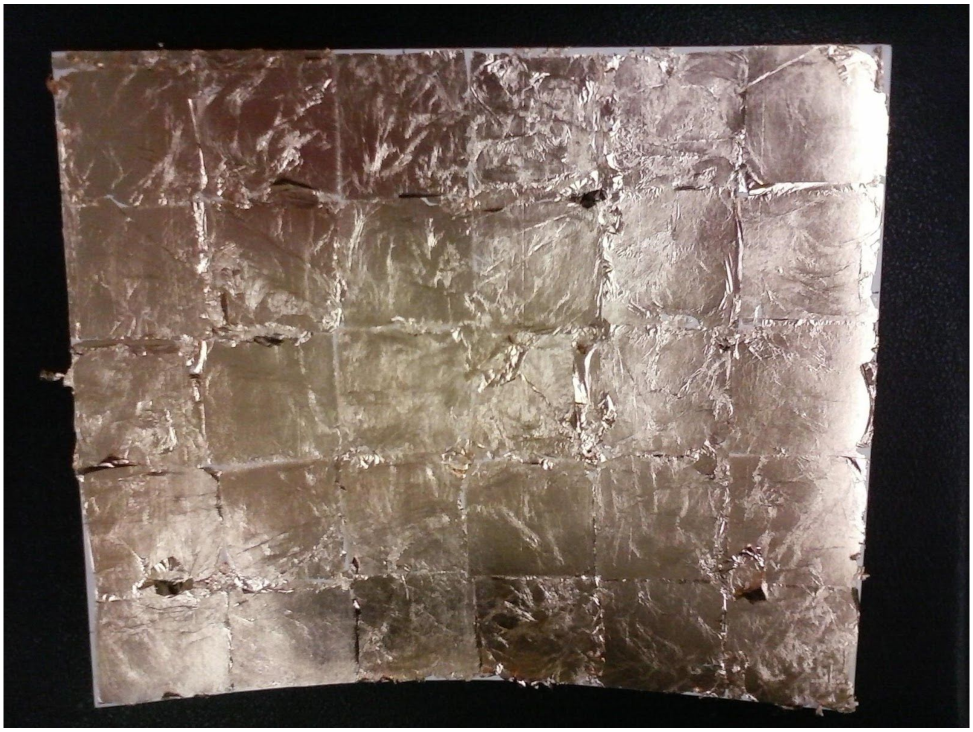

Image 17: Gold sheet

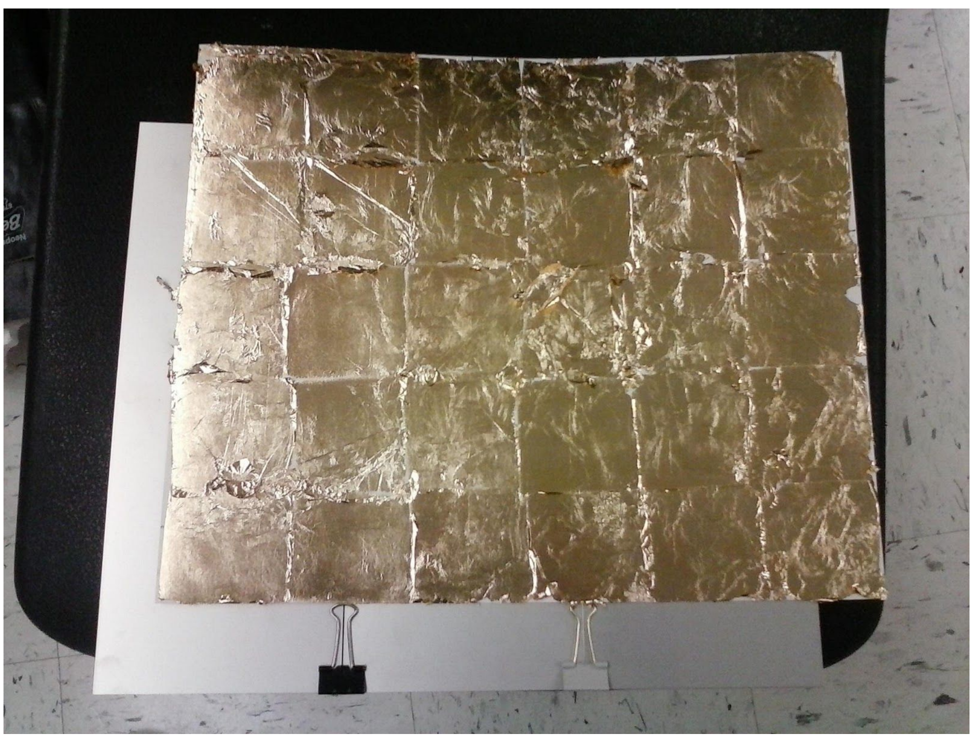

Image 18: Gold-Tin Layed sheet

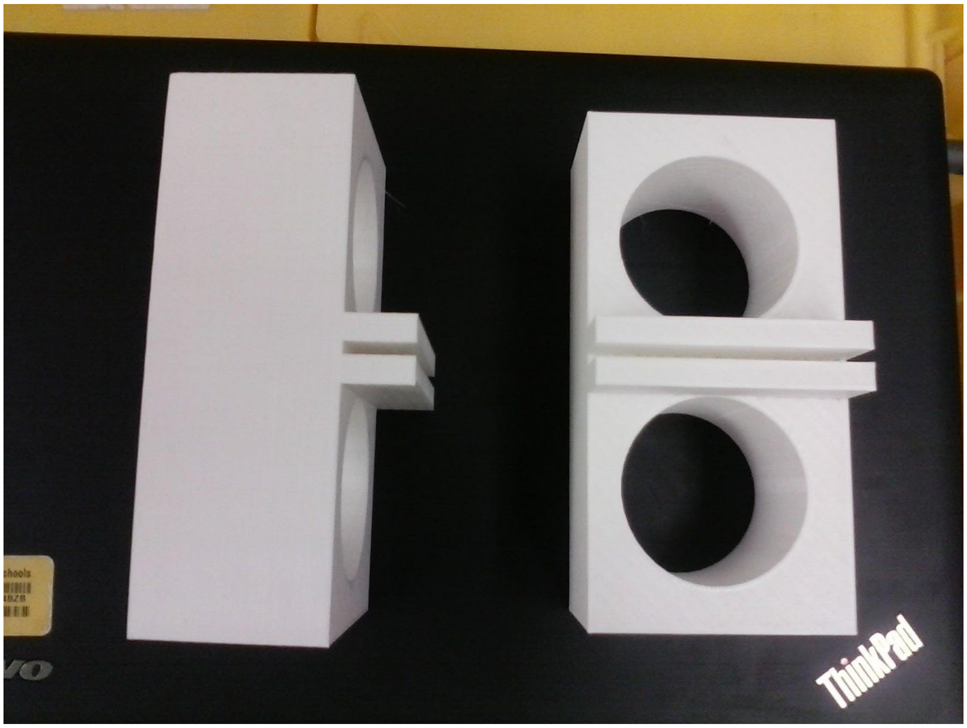

Image 19: Researcher's designed support system for detector paddles

Diagram 1: Solidworks Drawing of researcher's support system parts

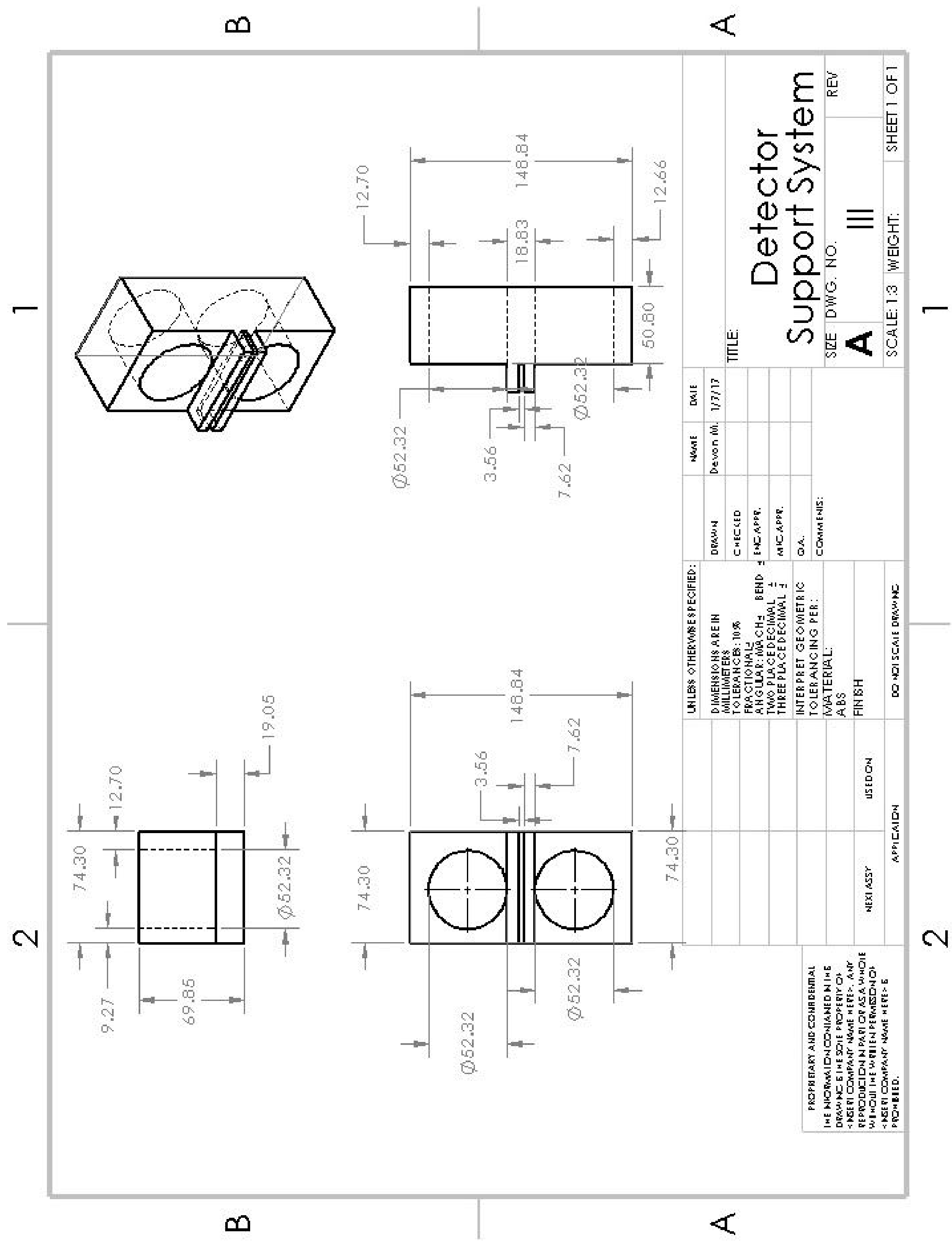

D. EXTRA GRAPHS (Developed from extra data collected after project)

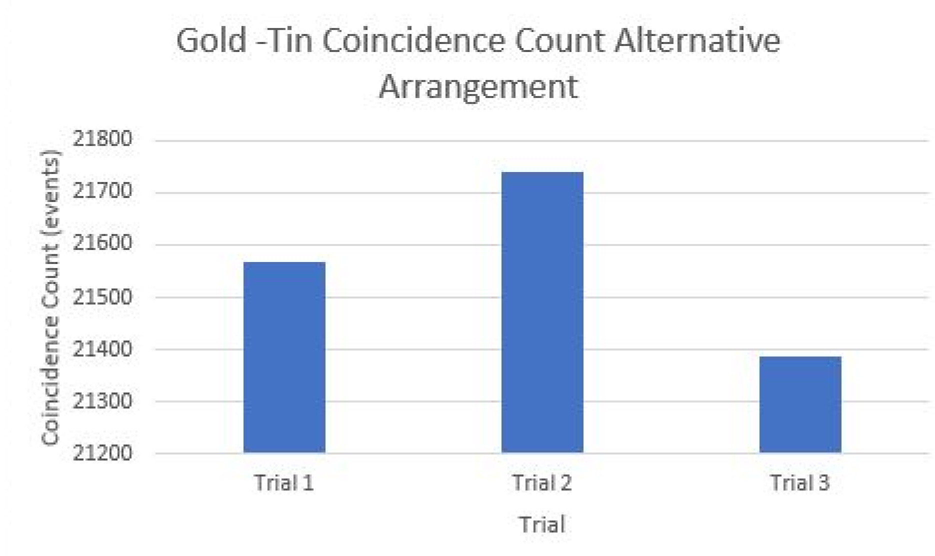

Graph 1: Gold tin trial with alternative arrangement in detector.

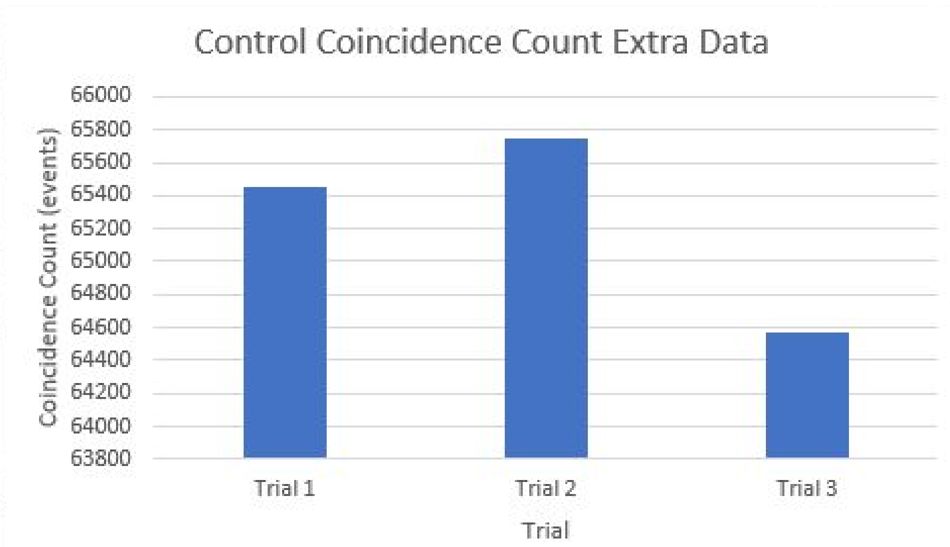

Graph 2: Control bar graph created from extra data collected.

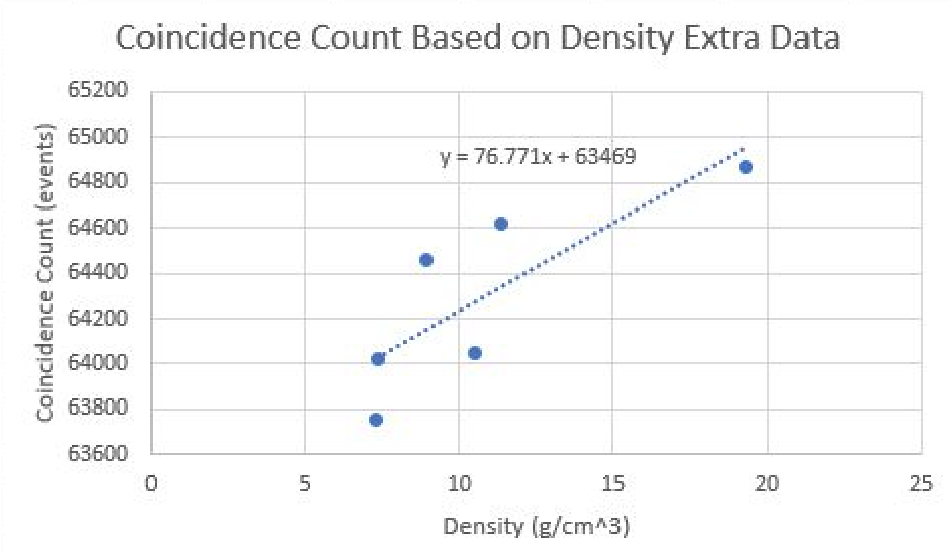

Graph 3: Scatter plot with line of best fit for Density versus Coincidence count from extra data collected.

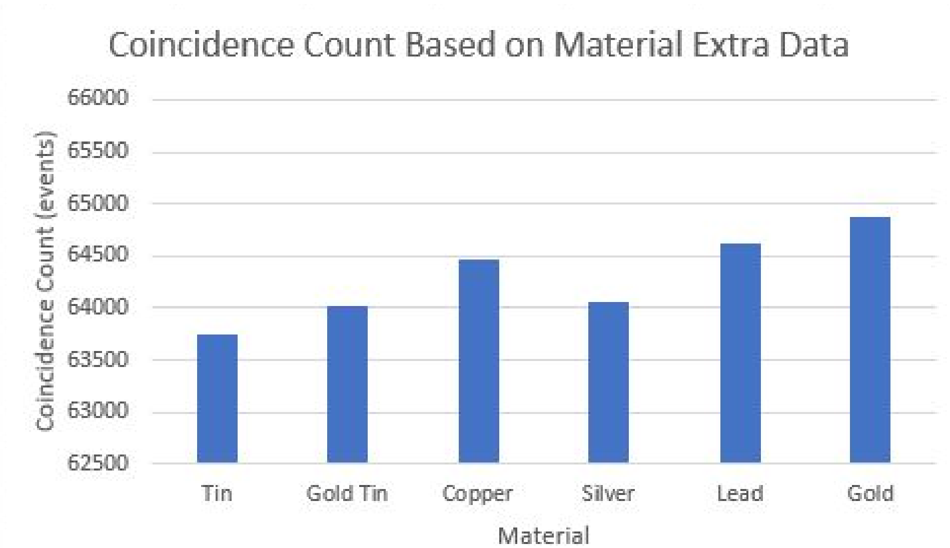

Graph 4: Bar graph of each material average coincidence count using extra data.

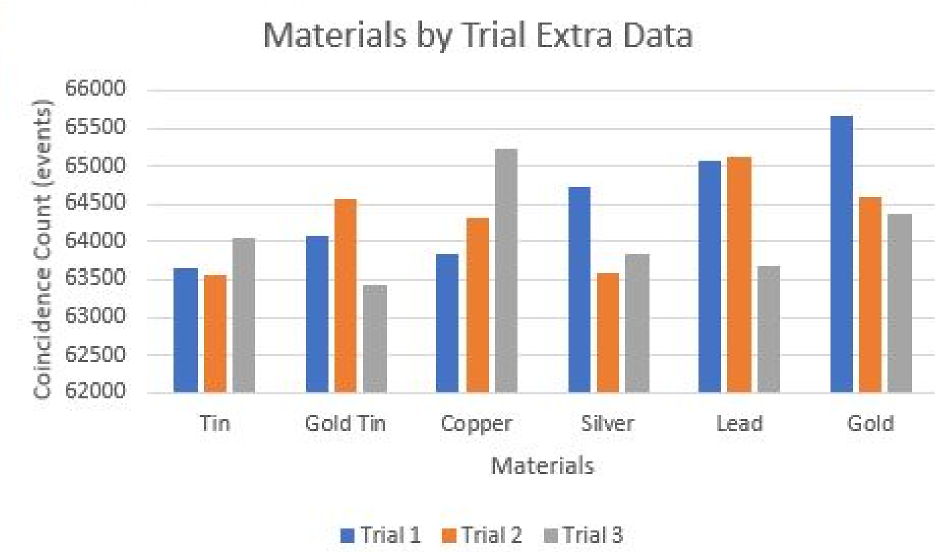

Graph 5: Materials separated by trial bar graph created using extra data collected.

Bibliography:

Adams, M. (2012). QuarkNet Cosmic Ray Muon Detector (CRMD) Assembly Instructions for Series 6000 DAQ. Fermi National Accelerator Laboratory, 1-10. Retrieved November 30, 2016, from https://quarknet.i2u2.org/sites/default/files/cf_crmdassemblyinstructions-small.pdf

Byun, S. (n.d.). Chapter 4 Scintillation Detectors. McMaster University, 4-1-4-10. Retrieved August 31, 2016, from https://www.science.mcmaster.ca/medphys/images/files/courses/4R06/note4.pdf

Cecire, K. (2002, March 22). Fermilab Detector. Retrieved August 30, 2016, from http://quarknet.fnal.gov/toolkits/new/fnaldet.html

Chemical elements listed by density. (n.d.). Retrieved June 27, 2016, from http://www.lenntech.com/periodic-chart-elements/density.htm

Cherry, J. D., Liu, B., Frost, J. L., Lemere, C. A., Williams, J. P., Olschowka, J. A., & O’Banion, M. K. (2012). Galactic Cosmic Radiation Leads to Cognitive Impairment and Increased Aβ Plaque Accumulation in a Mouse Model of Alzheimer’s Disease. PLoS ONE, 7(12), e53275. http://doi.org/10.1371/journal.pone.0053275

Cucinotta, F. A., Kim, M. Y., Chappell, L. J., & Huff, J. L. (2013). How Safe Is Safe Enough? Radiation Risk for a Human Mission to Mars. Plos ONE, 8(10), 1-9. doi:10.1371/journal.pone.0074988

Density of steel. (2016). Retrieved November 1, 2016, from http://www.thyssenkruppaerospace.com/nc/materials/steel/steel-sheet-plate/weight-calculations.html?print=1

Disposing of Lead Paint Waste. (n.d.). *Topics in Applied Chemistry Lead-Based Paint Handbook,* 11-11. doi:10.1007/0-306-46905-7_12

Fleetwood, D. M., & Winokur, P. S. (2000). Radiation effects in the space telecommunications environment. 22nd International Conference on Microelectronics. Proceedings (Cat. No.00TH8400), 1-8. doi:10.1109/icmel.2000.840529

Flux Study Tutorial. (n.d.). Retrieved February 14, 2017, from https://www.i2u2.org/elab/cosmic/analysis-flux/tutorial.jsp

Frazier, S. (2015, September 30). Real Martians: How to Protect Astronauts from Space Radiation on Mars. Retrieved December 12, 2016, from https://www.nasa.gov/feature/goddard/real-martians-how-to-protect-astronauts-from-space-radiation-on-mars

Galactic Cosmic Rays. (n.d.). Retrieved October 10, 2016, from http://www.swpc.noaa.gov/phenomena/galactic-cosmic-rays

How does lead absorb radiation like x-rays and gamma rays? (2009, November 29). Retrieved June 29, 2016, from http://www.thenakedscientists.com/HTML/questions/question/2490/

Kliewer, S. (n.d.). Primary Cosmic Rays. Retrieved October 10, 2016, from http://cosmic.lbl.gov/SKliewer/Cosmic_Rays/Primary.htm

Larson, R., & Farber, E. (2009). *Elementary statistics: Picturing the world* (6th ed.). Upper Saddle River, NJ: Pearson Prentice Hall.

Lofgren, J. (2001). Quarknet Cosmic Ray Detector System. Florida Institute of Technology, 1-18. Retrieved July 11, 2016, from http://research.fit.edu/quarknet/documents/Quarknet_card1_referenc.pdf

Material Safety Data Sheet: Lead, Metal. (2014). Carolina.com, 1-4. Retrieved September 25, 2016, from http://www.carolina.com/pdf/msds/leadgranshotghs.pdf

Ohnishi, T. (2016, April 29). Life science experiments performed in space in the ISS/Kibo facility and future research plans. Journal of Radiation Research, 57(S1), I41-I46. doi:10.1093/jrr/rrw020

Polyethylene (High Density) HDPE. (n.d.). Retrieved February 10, 2017, from http://www.bpf.co.uk/plastipedia/polymers/HDPE.aspx

Regulatory Affairs. (2010). Material Safety Data Sheet: Loctite Weld bonding Compound. Henkel Consumer Adhesives, 1-5. Retrieved October 26, 2016, from https://www.menards.com/msds/110155_001.pdf.

Siegel, P. (2015). Attenuation of Radiation in Matter. Physics Department California State Polytechnic University, 1-7. Retrieved December 5, 2016, from https://www.cpp.edu/~pbsiegel/bio431/texnotes/chapter6.pdf.

Solid Waste Management Staff. (n.d.). Solid Waste Management Department Household Hazardous Waste. Retrieved October 30, 2016, from http://www.brevardcounty.us/solidwaste/householdhazardouswaste

Space travel linked to Alzheimer's disease. (2013, February). The Science Teacher, 80(2), 13+. Retrieved from http://ic.galegroup.com/ic/suic/AcademicJournalsDetailsPage/AcademicJournalsDetailsWindow?disableHighlighting=false&displayGroupName=Journals&currPage=&scanId=&query=&prodId=SUIC&search_within_results=&p=SUIC&mode=view&catId=&limiter=&display-query=&displayGroups=&contentModules=&action=e&sortBy=&documentId=GALE%7CA320439389&windowstate=normal&activityType=&failOverType=&commentary=&source=Bookmark&u=fl_breva&jsid=809261c48ed2445980bba1a6a69de0da

Tripathi, R. K. (2011). Radiation Effects In Space. AIP Conference Proceedings, 1336(1), 649-654. doi:10.1063/1.3586182

Winter, M. (n.d.). Technetium: The essentials. Retrieved June 30, 2016, from https://www.webelements.com/technetium/